NPS-59SL74091

NAVAL POSTGRADUATE SCHOOL

Monterey, California

PERIODIC FLOW ABOUT BLUFF BODIES

PART-1

FORCES ON CYLINDERS AND SPHERES IN A SINUSOIDALLY OSCILLATING FLUID

TURGUT SARPKAYA

OLCAY TUTER

September 1974

Technical Report Period September 1973-1974

Approved for public release; distribution unlimited

Prepared for:

National Science Foundation, Washington, D. C. 20550

NAVAL POSTGRADUATE SCHOOL

Monterey, California

Rear Admiral Isham Linder
Superintendent

Jack B. Borsting
Provost

The work reported herein was supported by the National Science Foundation, Washington, D. C. 20550.

This report was prepared by:

R. H. Nunn, Chairman
Department of Mechanical Engineering

D. B. Hoisington
Acting Dean of Research

UNCLASSIFIED

SECURITY CLASSIFICATION OF THIS PAGE *(When Data Entered)*

REPORT DOCUMENTATION PAGE		READ INSTRUCTIONS BEFORE COMPLETING FORM
1. REPORT NUMBER NPS-59SL74091	2. GOVT ACCESSION NO.	3. RECIPIENT'S CATALOG NUMBER
4. TITLE *(and Subtitle)* Periodic Flow About Bluff Bodies. Part-1: Forces on Cylinders and Spheres in a Sinusoidally Oscillating Fluid.		5. TYPE OF REPORT & PERIOD COVERED September 1973-1974 6. PERFORMING ORG. REPORT NUMBER
7. AUTHOR(s) Turgut Sarpkaya & Olcay Tuter Sarpkaya		8. CONTRACT OR GRANT NUMBER(s) Grant No: AG-477 (NSF)
9. PERFORMING ORGANIZATION NAME AND ADDRESS Naval Postgraduate School Monterey. California 93940		10. PROGRAM ELEMENT, PROJECT, TASK AREA & WORK UNIT NUMBERS
11. CONTROLLING OFFICE NAME AND ADDRESS National Science Foundation Washington, D. C. 20550		12. REPORT DATE September 1974 13. NUMBER OF PAGES 89
14. MONITORING AGENCY NAME & ADDRESS*(if different from Controlling Office)*		15. SECURITY CLASS. *(of this report)* Unclassified 15a. DECLASSIFICATION/DOWNGRADING SCHEDULE

16. DISTRIBUTION STATEMENT *(of this Report)*

Approved for public release; Distribution unlimited.

17. DISTRIBUTION STATEMENT *(of the abstract entered in Block 20, if different from Report)*

18. SUPPLEMENTARY NOTES Part of the results have been presented at the 14th International Conference on Coastal Engineering, Copenhagen Denmark, June 24-28, 1974.

19. KEY WORDS *(Continue on reverse side if necessary and identify by block number)*

Oscillating flow, Wave forces, Drag and inertia coefficients. Cylinders and spheres in an oscillating flow.

20. ABSTRACT *(Continue on reverse side if necessary and identify by block number)*

The in-line and transverse forces acting on cylinders and the in-line force acting on spheres placed in a sinusoidally oscillating fluid have been measured. The periodic flow was generated in a U-shaped vertical water channel through the use of a pneumatic oscillator.

DD FORM 1 JAN 73 1473 EDITION OF 1 NOV 65 IS OBSOLETE
S/N 0102-014-6601 |

UNCLASSIFIED

SECURITY CLASSIFICATION OF THIS PAGE *(When Data Entered)*

The drag, inertia and the lift coefficients as well as the total force coefficient have been determined through the use of Fourier analysis and found to depend on a period parameter.

The results have shown that the transverse force acting on a cylinder in a periodic flow with zero mean velocity is as large as the in-line force. The frequency of the alternating transverse force depends on a period parameter and several frequencies may occur during a given period of oscillation of the flow.

It is recommended that the experiments be extended to Reynolds numbers as large as 10^6 in a similar but larger apparatus.

TABLE OF CONTENTS

LIST OF FIGURES

Figure

Figure

NOMENCLATURE

A	amplitude of the motion
C_D	average drag coefficient
C_M	average inertia coefficient
C_{LMAX}	maximum lift coefficient
C_T	maximum total force coefficient
d	diameter of test cylinder
F	instantaneous total force acting on the test cylinder
F_D	drag force acting on the test cylinder
F_L	lift force acting on the test cylinder
F_{LMAX}	maximum lift force acting on the test cylinder
l	length of test cylinder
Re	Reynolds number ($Re = Vd/\nu$)
T	period of oscillation
t	time
V	instantaneous velocity
V_m	maximum velocity
λ	percent error
λ^*	percent error based on maximum forces
ν	fluid kinematic viscosity
ρ	fluid density
Φ	phase angle

ACKNOWLEDGEMENT

The work described in this report represents part of a research program supported by the Engineering Division of the National Science Foundation.

It is a pleasure to acknowledge the help given by Messrs. K. Mothersell, J. McKay, and T. F. Christian of the machine shop of the Department of Mechanical Engineering in constructing the test facilities.

I. INTRODUCTION

A. EXPERIMENTAL JUSTIFICATION

The subject of forces acting on bluff bodies immersed in time-dependent flows has been and will continue to be of interest to fluid dynamicists, aerodynamicists, and practicing engineers for the special reason that in nature neither the body nor the fluid which surrounds the body is ever in a state of steady motion. Even the flow behind a bluff body moving steadily through a fluid is accompanied by large scale unsteadiness. Thus, any type of unsteadiness of the ambient flow and/or the motion of the body introduces additional changes in the characteristics of the flow and its analysis.

The drag and inertial forces are interdependent as well as time dependent, and the resistance coefficients obtained in unseparated flows are not applicable to separated cases. Although indirect, the role of viscosity is paramount in that its consequences are separation, vortex formation and shedding, and resultant alternations in the virtual mass. It is thus clear that it is necessary to determine the relationships between various resistance components in terms of the unsteadiness of the ambient flow and/or body motion, geometry of the body, the degree of upstream turbulence, past history of the flow, etc. [Ref. 1].

However, the understanding of the behavior of time-dependent flows about bluff bodies may be advanced only by considering the relatively more manageable cases and gradually

integrating the information so obtained. This led to the present experimental investigation of the harmonically oscillating flow about circular cylinders and spheres.

B. SURVEY OF THE PREVIOUS INVESTIGATIONS

A review of some of the previous investigations on time-dependent flows may best be presented by dividing the motions under consideration into various but admittedly arbitrary categories.

1. Theoretical Analysis of Unseparated Time-Dependent Laminar Flows

The study of the theory of separation-free time-dependent laminar flows has enjoyed particular attention, partly due to its practical significance and partly due to its relative mathematical simplicity. Surveys by Stewartson [Ref. 2], Stuart [Ref. 3], and Rott [Ref. 4] reflect the current level of understanding.

The unseparated class of unsteady flows, most of which results from the unidirectional or periodic acceleration of bodies in an infinite or bounded fluid medium, gives rise to an induced mass which must be added to the real mass of the body. In general, the virtual inertia tensor depends on the shape of the body, the nature of the fluid medium, the orientation of the moving object with respect to the direction of motion, and the depth of relative submergence from a free surface and/or solid boundary.

The effects of viscosity and separation on added mass or the dependence of added mass of a given body on the

characteristics of the time-dependent separated flow cannot yet be theoretically evaluated nor can it be experimentally separated from the total resistance experienced by the body.

2. Small Amplitude Vibration of Bodies in a Liquid Otherwise at Rest and the Initial Instants of Acceleration of Bodies from a State of Uniform Velocity

Vibratory motion has often been used [Refs. 5-8] as one of the experimental means to determine the virtual mass coefficients. The technique has been restricted to amplitudes of motion which are so small that either separation does not occur or the characteristics of separation do not change due to the imposed, high-frequency vibration. Thus, the results obtained are not applicable to occurrences in which the duration of unsteady flow in one direction is long enough for separation to occur.

It is not necessary that the body be initially at rest to determine the added mass provided that one starts with a steady ambient flow about the body or with the body moving at constant velocity in a fluid otherwise at rest. Hamilton and Lindell [Ref. 9] have shown that the added-mass coefficient of a sphere determined by imposing a uniform acceleration onto its steady state motion is equal to its theoretically determined value as well as to its experimentally determined value obtained by small-amplitude, high-frequency oscillations.

Rayleigh [Ref. 10] has shown that if the acceleration continues, i.e. $V = \overline{V} + kt^m$, both the drag and the added-mass coefficients change with time.

The foregoing arguments suggest that the force exerted by the fluid on a body immersed in a time-dependent flow might be expressed as

$$F = \tfrac{1}{2}C_D\rho A|\bar{V}|\bar{V} + C_M m_f \, dV/dt + \text{history-dependent} \qquad (1)$$

drag and inertia forces

in which A is the projected area of the body and m_f the mass of the fluid displaced by the body. The drag coefficient C_D is to be taken equal to the quasi-steady state resistance coefficient and C_M to be taken equal to that measured or calculated from the potential theory when the value of the history-dependent force is zero [Ref. 9].

3. Bodies Subjected to Large Amplitude Harmonic Oscillations in a Fluid Otherwise at Rest

A number of significant studies [Refs. 11-16] were made to determine the forces acting on bluff bodies undergoing harmonic, large-amplitude oscillations in a liquid otherwise at rest.

Odar and Hamilton [Ref. 11] measured the force acting on a sphere subjected to harmonic oscillations and proposed a force equation comprised of three parts: a steady drag component where the drag coefficient is the well-established coefficient for steady translation of a sphere; an inertial component whose coefficient is determined experimentally as a function of V^2/ad (a: acceleration; d: diameter of sphere); and a history-dependent component whose coefficient also is a function of V^2/ad.

4. Bodies Subjected to Wave Motion with Zero Mean Velocity

Considerable work [Refs. 17-23] has been done on this type of time-dependent flow in an attempt to predict the wave forces on piles and other submerged structures. In general, the total force acting on the body is assumed to be composed of a velocity-dependent and an acceleration-dependent force. The resulting equation, known as the Morison equation [Ref. 16], is given by

$$F = \tfrac{1}{2}C_D\rho A|\overline{V}|\overline{V} + C_M m_f \, dV/dt \qquad (2)$$

where $C_M = 1+C$, C being the added mass coefficient. Experiments show that C_D and C_M depend on time and show considerable scatter about their assumed mean values [Refs. 18, 21] over a cycle.

5. Bodies Subjected to Unidirectional Acceleration in a Fluid Otherwise at Rest or Unidirectional Unsteady Flow About Bodies Held at Rest

Substantial effort has been made to determine the components of force acting on a body accelerating unidirectionally in a fluid otherwise at rest. Iverson and Balent [Ref. 24] and Keim [Ref. 25] towed spheres, disks, and cylinders in unsteady motion through still water. It was concluded that the total instantaneous force on these objects could be described by a single coefficient of the form $C = 2F/\rho AV^2$ and that this coefficient was a function only of a so-called acceleration modulus, ad/V^2. Keim, however, detected an apparent Reynolds number effect for cylinders.

Laird et. al. [Ref. 26] measured the forces acting on accelerating cylinders and found strong evidence of deviation of the drag coefficient from the accepted values for uniform motion. They further found that the acceleration modulus did not correlate the resistance coefficient near boundary-layer transition.

Sarpkaya and Garrison [Ref. 27] working with unidirectional flow with constant acceleration about cylinders and plates have found that both C_D and C_M depend on the history of motion, that the Morison equation (Eq. 2) is valid only for flows with constant acceleration, and that the acceleration modulus can correlate the data only if the acceleration is kept constant.

6. Forced or Self-Induced Transverse Oscillations of a Body in a Fluid in Steady Motion

Experiments have been directed to the effects that attend the oscillations of a body in the plane of the lift force. This type of interaction becomes particularly important when the oscillation of the structure is the necessary condition for the generation of the exciting forces. The most pertinent information from these experiments is that the lift and drag forces act on the oscillating cylinder at the vortex shedding frequency and twice the shedding frequency, respectively, provided that the driving frequency on the cylinder is appreciably different from the shedding frequency. When the forcing frequency of the cylinder approaches the shedding frequency, the natural shedding frequency is

lost and it "locks-in" to the forcing frequency. This synchronization persists over a range of frequencies which may be termed the "range of synchronization" [Ref. 28].

7. Unidirectional Oscillatory Flow About Bodies at Rest and Steady Uniform Flow About Bodies Subjected to Streamwise Oscillations

Relatively few studies have been conducted in this category. Chan and Ballengee [Ref. 29] examined the vortex shedding from circular cylinders in an oscillating free stream. Their results suggested that "in an oscillatory freestream of 3 HZ and Reynolds number up to 40,000, the vortex shedding from a circular cylinder responds instantaneously to the freestream variations" and that "the instantaneous Strouhal number stays sensibly constant at 0.2 ± 0.01."

Hatfield and Morkovin [Ref. 30] studied the effect of an oscillating freestream on the unsteady pressure on a circular cylinder. They have found that there is no significant coupling between the small-amplitude freestream oscillations and the vortex shedding. Their results would suggest that the drag coefficient associated with the mean flow would essentially remain constant at its steady state value. On the other hand, Mercier [Ref. 31] who subjected cylinders to large streamwise oscillations found that the average drag coefficient significantly increases with fd/V and that the rate of increase depends on the amplitude to diameter ratio. Combined, these results would suggest that the degree of coupling between the frequency of oscillation and the vortex-shedding frequency and hence the forces acting on the body strongly depend on the amplitude of oscillation.

Davenport [Ref. 32] subjected bluff bodies to small amplitude oscillations in a water flume and evaluated the drag and inertia coefficients through the measurement of the rate of damping of the amplitude of oscillations of the bodies, i.e. without measuring the forces acting on the bodies. Using the frequency parameter $fd/\overline{V}$ to correlate the data, he found large variations in C_D and C_M.

C. SCOPE OF THE PRESENT STUDY

The present investigation is limited to an experimental investigation of the drag, inertia, and lift forces acting on circular cylinders and the drag and inertia forces acting on spheres immersed in a periodically oscillating fluid with zero mean velocity. The fluid motion is characterized by

$$V = -V_m \cos \frac{2\pi}{T} t \qquad (3)$$

where V_m is the maximum velocity, T the period of the oscillation, and V the instantaneous velocity.

As noted earlier, this type of fluid motion about cylinders and plates has been studied by Keulegan and Carpenter [Ref. 18] through the use of standing waves in a rectangular basin. The characteristics of the ambient fluid motion have been determined through the use of the appropriate standing-wave equations and the measured amplitude of the waves. Keulegan and Carpenter determined the drag and inertia coefficients and correlated them with the so-called period parameter V_mT/d. They have found that the Fourier-averaged values of the inertia and drag coefficients over a wave

cycle show considerable variations with $V_m T/d$. For cylinders $V_m T/d$ equalling 15 was found to be a critical condition yielding the lowest value of the inertia coefficient and the largest value of the drag coefficient. For the plates the higher values of the drag coefficient are associated with the smaller values of $V_m T/d$ and the higher values of the inertia coefficient with the larger values of $V_m T/d$. It was suggested by Keulegan and Carpenter that the parameter $V_m T/d$, or equivalently, the relative fluid displacement A/d was the parameter of primary importance and the effect of Reynolds number was assumed to be of little importance on the values of the drag and inertia coefficients. It is noted, however, that the test method used by Keulegan and Carpenter allowed no control over the Reynolds number so that they had no convenient method of testing this influence. Finally, it should also be noted that Keulegan and Carpenter did not measure the lift forces acting on cylinders.

Driscoll [Ref. 16] oscillated circular cylinders in simple harmonic motion in water otherwise at rest and found that the inertia coefficient is almost independent of the Reynolds number and highly dependent upon A/d and that the drag coefficient is strongly affected by the Reynolds number and generally it decreases with increasing Reynolds number.[1]

---

[1] Driscoll's [Ref. 16] C_M and C_D values are in error since the length of the test cylinder was inadvertantly taken as unity in the calculations instead of its actual length of 1.375 inches.

The lift force averaged over the length of a circular pile was measured by Bidde [Ref. 33]. He found that the maximum values of the lift coefficient expressed by

$$F_{LMAX} = \tfrac{1}{2}\rho V_m^2 \, d\rho C_{LMAX} \qquad (4)$$

reaches 60% of the longitudinal force for the rigid pile used and that C_{LMAX} has a maximum average value of about 1.5. His data showed considerable scatter over the range of V_mT/d values encountered in the experiments. Nevertheless, C_{LMAX} showed a better correlation with V_mT/d than with the Reynolds number. This study does not shed much light on the understanding of the variation of the lift coefficient with either parameter since the lift varies along the pile in accordance with the characteristics of the wave motion.

Rance [Ref. 34] investigated the drag, inertia and lift forces acting on cylinders placed in an oscillating-flow water tunnel and found that the lift coefficient may reach values as high as 2.0. He did not attempt to correlate his results with the period parameter. Rance concluded that the lift force appeared to be significant compared with the sum of the drag and inertia forces and that a combination of all the forces should be used in a practical design.

Relatively few studies have been carried out on wave forces on submerged spheres. Grace and Casciano [Ref. 35] measured wave forces on a subsurface sphere and was able to evaluate only the drag coefficient which ranged from 0.3 to 1.05. The data and the method of calculation did not allow

them to obtain either a systematic variation of C_D with the period parameter or to evaluate C_M.

It is evident from the foregoing summary of the previous studies on unsteady flows in general and of the simple harmonic motions about cylinders in particular that the questions regarding the determination of the lift, drag, and inertial forces for various types of bluff bodies immersed in periodic flows remain largely unresolved. There are several reasons for the difficulties encountered. Theoretically, the problem is not manageable because of the unsteadiness of the flow and the indeterminate nature of the separation points. Experimentally the difficulties stem from various sources in experiments. With oscillating bodies, the force resulting from the acceleration of the body must be separated by calculations. In the case of body immersed in an oscillating fluid, the characteristics of the fluid motion have often been evaluated through the use of approximate wave equations rather than measuring them directly. Furthermore, either in the case of body oscillations or in the case of fluid oscillations, the motion was not entirely harmonic. This, as well as the ever present ocean currents, may have led to large scatter in the data presented in the references cited. Thus the values of C_M and C_D so derived are associated uniquely with the particular wave theory used to determine their numerical values. In general, attempts to use these values with other wave theories may result in large errors. Finally, it should be mentioned that the values of C_M and C_D

which have been derived for cylinders placed horizontally in an oscillating fluid has often been identified in engineering usage with similar coefficients obtained from tests relating to vertical cylinders. Obviously, the characteristics of the wave motion as well as the bottom- and free-surface effects will significantly affect the variation of these coefficients with the significant parameters of the phenomenon.

The foregoing reasons, along with related aspects of the problem gave rise to questions concerning the validity of the methods for the prediction of forces acting on bluff bodies immersed in periodic flows. The present investigation is undertaken for the purpose of clarifying some of these problems through the use of a truly harmonic motion and to determine the drag, inertia, and the lift forces acting on cylinders and the drag, and inertia forces acting on spheres.

II. METHOD OF ANALYSIS

The total force acting on cylinders and spheres in the direction of the ambient fluid motion is assumed to be comprised of a drag force and an inertial force in the manner similar to that first suggested by Morison et. al. [Ref. 17]. For a cylinder it may be written as

$$F = \tfrac{1}{2}C_D\rho d\ell|V|V + C_M \frac{\pi d^2}{4} \rho\ell \frac{dV}{dt} \tag{5}$$

where F is the force for the length ℓ, d the diameter of the body, ρ the density of fluid, and V is the instantaneous velocity of the fluid. The C_D and C_M represent respectively the drag and inertia coefficients.

The corresponding equation for the sphere may be written as

$$F = \tfrac{1}{2}C_D\rho\frac{\pi d^2}{4}|V|V + C_M \frac{\pi d^3}{6} \rho \frac{dV}{dt} \tag{6}$$

in which F is the total force acting on the sphere.

The velocity of the ambient flow is represented by

$$V = -V_m \cos \sigma t \tag{7}$$

where V_m denotes the maximum velocity, T the period, and $\sigma = 2\pi/T$. The total force acting on the cylinder per unit length is in general given by

$$F = f(t,T,V_m,d,\rho,\nu) \tag{8}$$

Grouping the variables on the basis of dimensional reasoning and introducing $\alpha = 2\pi t/T$ gives

$$\frac{F}{V_m^2 d} = f(\alpha, \frac{V_m T}{d}, \frac{V_m d}{\nu}) \tag{9}$$

where $V_m d/\nu$ is a Reynolds number and $V_m T/d$, which can also be expressed as $2\pi A/d$, will be termed the relative displacement.

Because of flow symmetry and the periodic nature of the force

$$F(\alpha) = -F(\alpha+\pi) \tag{10}$$

it is possible to express the force coefficient in a Fourier series.

$$\frac{F}{V_m^2 d} = A_1 \sin \alpha + A_3 \sin 3\alpha + A_5 \sin 5\alpha + \ldots + B_1 \cos \alpha + B_3 \cos 3\alpha + B_5 \cos 5\alpha + \ldots \tag{11}$$

where the coefficients A_N, B_N are independent of α and at most functions of Reynolds number and relative displacement. Fourier analysis may be used to determine the coefficients as:

$$A_N = \frac{1}{\pi} \int_0^{2\pi} \frac{F \sin N\alpha}{\rho V_m^2 d} \, d\alpha \tag{12}$$

and

$$B_N = \frac{1}{\pi} \int_0^{2\pi} \frac{F \cos N\alpha}{\rho V_m^2 d} \, d\alpha \tag{13}$$

Once obtained, the dependence of these coefficients on Reynolds number and relative displacement may be established provided the data are sufficient.

The general formulation, equation (11), may be reconciled with Morison's equation (5). Introducing V from equation (7) into equation (5)

$$\frac{F}{\rho V_m^2 d} = \frac{\pi}{4} C_M \frac{d\sigma}{dm} \sin \alpha - \frac{C_D}{2} |\cos \alpha| \cos \alpha \qquad (14)$$

By the rule of Fourier

$$|\cos \alpha| \cos \alpha = \sum_{N=0}^{\infty} \frac{\int_0^{2\pi} |\cos \alpha| \cos \alpha \cos N\alpha d\alpha}{\int_0^{2\pi} \cos^2 N\alpha d\alpha}$$

$$= a_0 + a_1 \cos \alpha + a_2 \cos 2\alpha + a_3 \cos 3\alpha + \ldots$$

where

$$a_{even} = 0, \quad a_{odd} = (-1)^{\frac{N+1}{2}} \frac{8}{N(N-4)\pi} \qquad (15)$$

The first three non-zero coefficients would then be:

$$a_1 = 8/3\pi, \quad a_3 = 8/15\pi, \quad a_5 = 8/105\pi \qquad (16)$$

Introducing equation (16) into equation (11) with

$$B_1' = B_1/a_1$$
$$B_3' = B_3 - a_3/a_1(B_1)$$
$$B_5' = B_5 - a_5/a_1(B_1) \qquad (17)$$

yields

$$\frac{F}{\rho V_m^2 d} = A_1 \sin \alpha + A_3 \sin 3\alpha + A_5 \sin 5\alpha + \ldots$$
$$+ B_1' |\cos \alpha| \cos \alpha + B_3' |\cos 3\alpha| \cos 3\alpha$$
$$+ B_5' |\cos 5\alpha| \cos 5\alpha \qquad (18)$$

Equations (18) and (11) may be compared. Writing

$$\frac{\pi}{4} C_M \frac{d\sigma}{V_m} = A_1 + A_3 \frac{\sin 3\alpha}{\sin \alpha} + A_5 \frac{\sin 5\alpha}{\sin \alpha} + \ldots \qquad (19)$$

and

$$\frac{C_D}{2} = -B_1' - \frac{B_3' \cos 3\alpha}{|\cos\alpha|\cos\alpha} - \frac{B_5' \cos 5\alpha}{|\cos\alpha|\cos\alpha} + \ldots \qquad (20)$$

Thus, if the coefficients A_3, A_5 and B_3', B_5' vanish, the values of C_M and C_D remain constant for all phases of the cylinder motion

$$C_M = \frac{2}{\pi^2} \frac{V_m T}{d} A_1 \qquad (21)$$

Substituting A_1 from equation (12) yields

$$C_M = \frac{2}{\pi^2} \frac{V_m T}{d} \int_0^{2\pi} \frac{F \sin\alpha d\alpha}{\rho V_m^2 d} \qquad (22)$$

$$C_D = -2B_1' \qquad (23)$$

substituting from equations (13) and (17) yields

$$C_D = -\frac{3}{4} \int_0^{2\pi} \frac{F \sin\alpha d\alpha}{\rho V_m^2 d} \qquad (24)$$

If the coefficients do vary with the phase α, the values given by equations (22) and (24) are weighted averages. With this possibility in mind it is preferable to adopt

$$\frac{F}{\rho V_m^2 d} = A_1 \sin\alpha + B_1' \cos\alpha|\cos\alpha| + \text{error} \qquad (25)$$

or

$$\frac{F}{\rho V_m^2 d} = \frac{\pi}{4} C_M \frac{d\sigma}{V_m} \sin\alpha - \frac{C_D}{2}|\cos\alpha|\cos\alpha + \text{error} \qquad (26)$$

where A_1, B_1', C_M and C_D are constant and error has the value

$$\text{error} = A_3 \sin 3\alpha + A_5 \sin 5\alpha + B_3' \cos 3\alpha + B_5' \cos 5\alpha$$

This error may be obtained by subtracting the computed value of $A_1 \sin \alpha$ and $B_1' |\cos \alpha| \cos \alpha$ from the observed $F/\rho V_m^2 d$.

The foregoing formulation was developed by Keulegan and Carpenter [Ref. 18] and equations (22) and (24) were the basis for the computer data reduction programs.

For this purpose equations (22) and (24) were written as follows

$$C_M = \frac{2T^2}{\pi^3 d^2 \ell \rho A} \Sigma F \sin \left(\frac{2\pi t}{T}\right) \delta\left(\frac{t}{T}\right) \tag{27}$$

and

$$C_D = \frac{-3T^2}{8\rho d \pi \ell A^2} \Sigma F \cos \left(\frac{2\pi t}{T}\right) \delta\left(\frac{t}{T}\right) \tag{28}$$

The corresponding coefficients for the sphere may be obtained through the use of equation (6) and through the use of a similar Fourier analysis. The results are given by

$$C_M = \frac{3T^2}{\pi^3 d^3 \rho A} \Sigma F \sin \left(\frac{2\pi t}{T}\right) \delta\left(\frac{t}{T}\right) \tag{29}$$

and

$$C_D = \frac{-3T^2}{2\rho \pi^2 d^2 A^2} \Sigma F \cos \left(\frac{2\pi t}{T}\right) \delta\left(\frac{t}{T}\right) \tag{30}$$

The error in force predictions or the difference between the measured and the calculated forces acting on cylinders and spheres have been calculated not through the use of equation (26) but rather through the use of the following expression:

$$\text{Percent Error} = \frac{F_{mes} - F_{cal}}{(F_{mes})_{max}} \tag{31}$$

in which F_{mes} is the measured force and F_{cal} is the calculated force. It is thought that the percent error calculated in this manner will be physically more meaningful than the predicted error given by equation (26).

Computer programs have been devised for the evaluation of the coefficients given by equations (27), (28), (29), and (30). These programs are presented in Appendix A.

Finally the maximum lift coefficient for each $V_m T/d$ has been calculated through the use of

$$C_{LMAX} = \frac{F_{LMAX}}{\frac{1}{2}\rho d \ell V_m^2} \tag{32}$$

in which F_{LMAX} is the maximum lift force in a given cycle for a given $V_m T/d$. The corresponding computer program for C_{LMAX} is also given in Appendix A. No attempt was made to separately analyze the amplitudes of the harmonics of the lift force.

III. EXPERIMENTAL EQUIPMENT AND PROCEDURE

A. EQUIPMENT

The basic oscillating flow system consisted of a U-shaped vertical water channel. The cross-section of the test section was 18 by 20 inches. A photograph of the equipment and a schematic drawing of the channel are shown in figures 1 and 2. The test bodies were mounted 2.5 feet below the free surface of the still water level. The fluid in the U-channel was oscillated pneumatically through the use of a slider-crank mechanism which has periodically opened and closed the air supply line and also a large exit hole at the top of one of the legs of the channel. A photograph of the oscillating mechanism is shown in fig. 3.

The frequency of oscillation of the slider-crank mechanism was matched to the natural frequency of oscillation of the water column in the channel by means of reduction gears and through the use of a variable speed DC motor. The maximum half-amplitude of oscillation of water column was 11 inches and the natural damping of the oscillations was in the order of 1/8 inch per cycle without the use of the pneumatic pulsating system. The water level at its minimum height in the test section was about 20 inches above the test body. The cylinders were manufactured out of plexiglass tubes or rods at desired diameters and at lengths approximately 1/16 inch under the width of the test section. Self-aligning bearings were imbedded at each end of the cylinders.

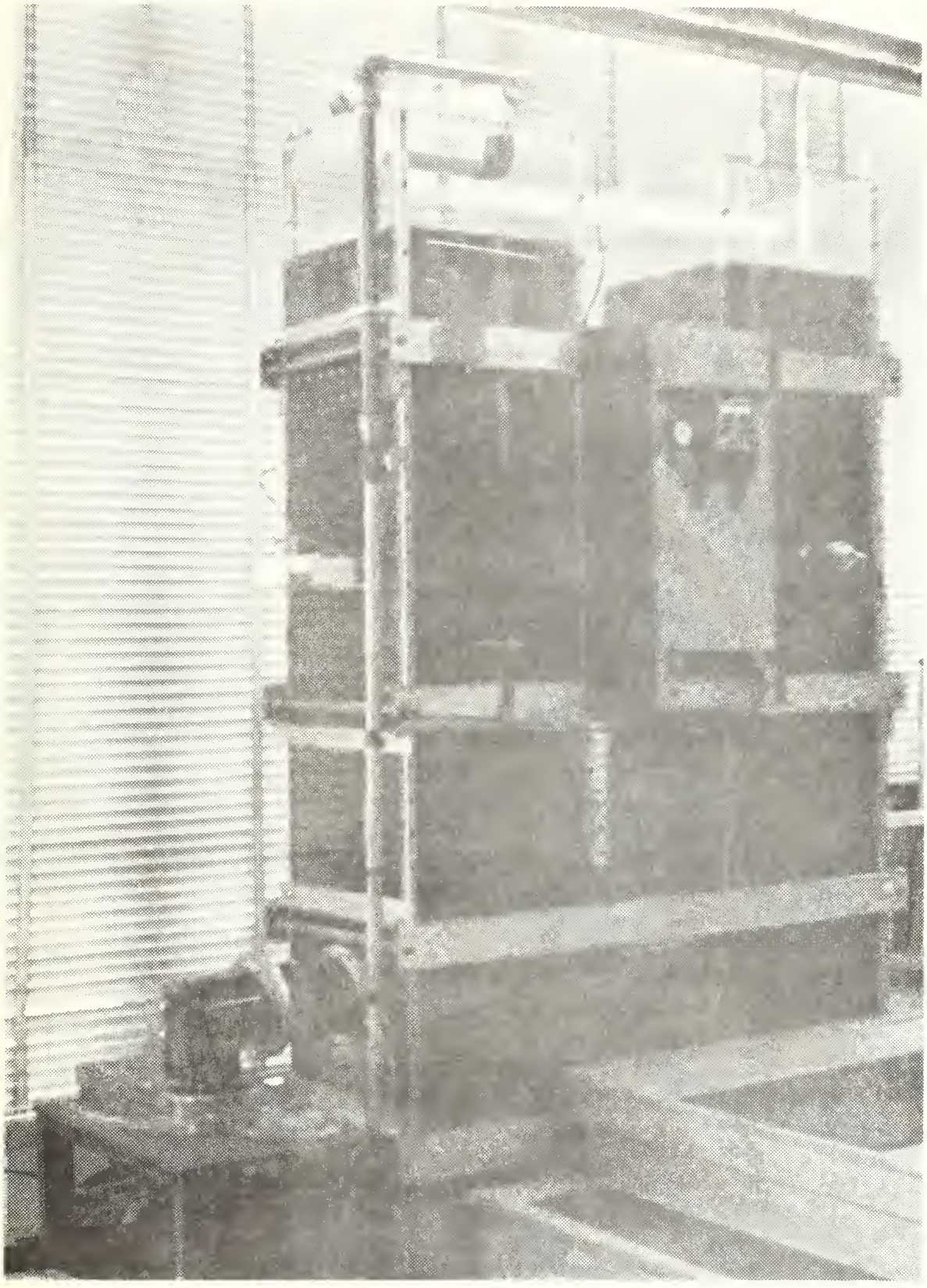

Figure 1. U-Channel

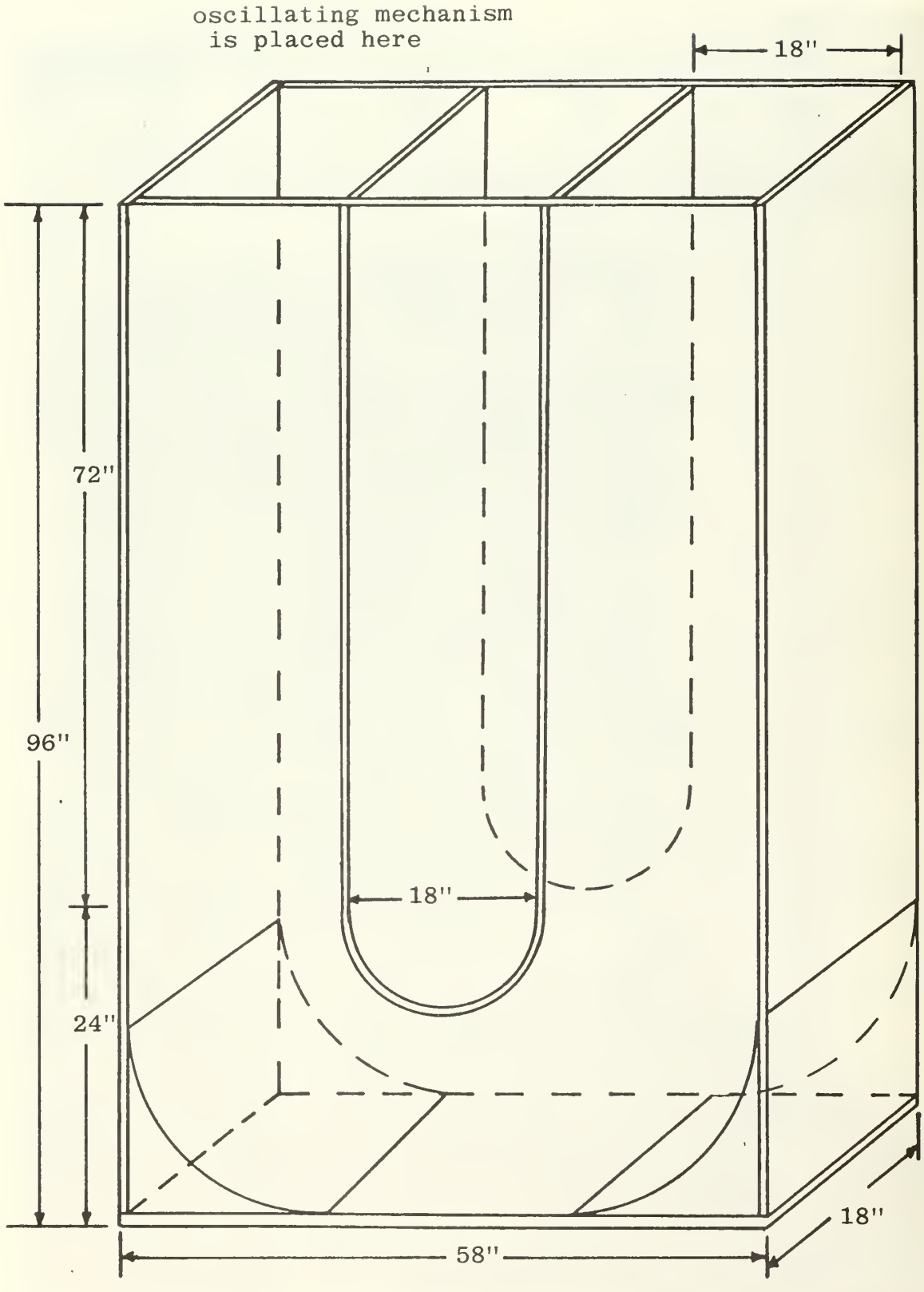

Figure 2. Schematic drawing of the U-channel

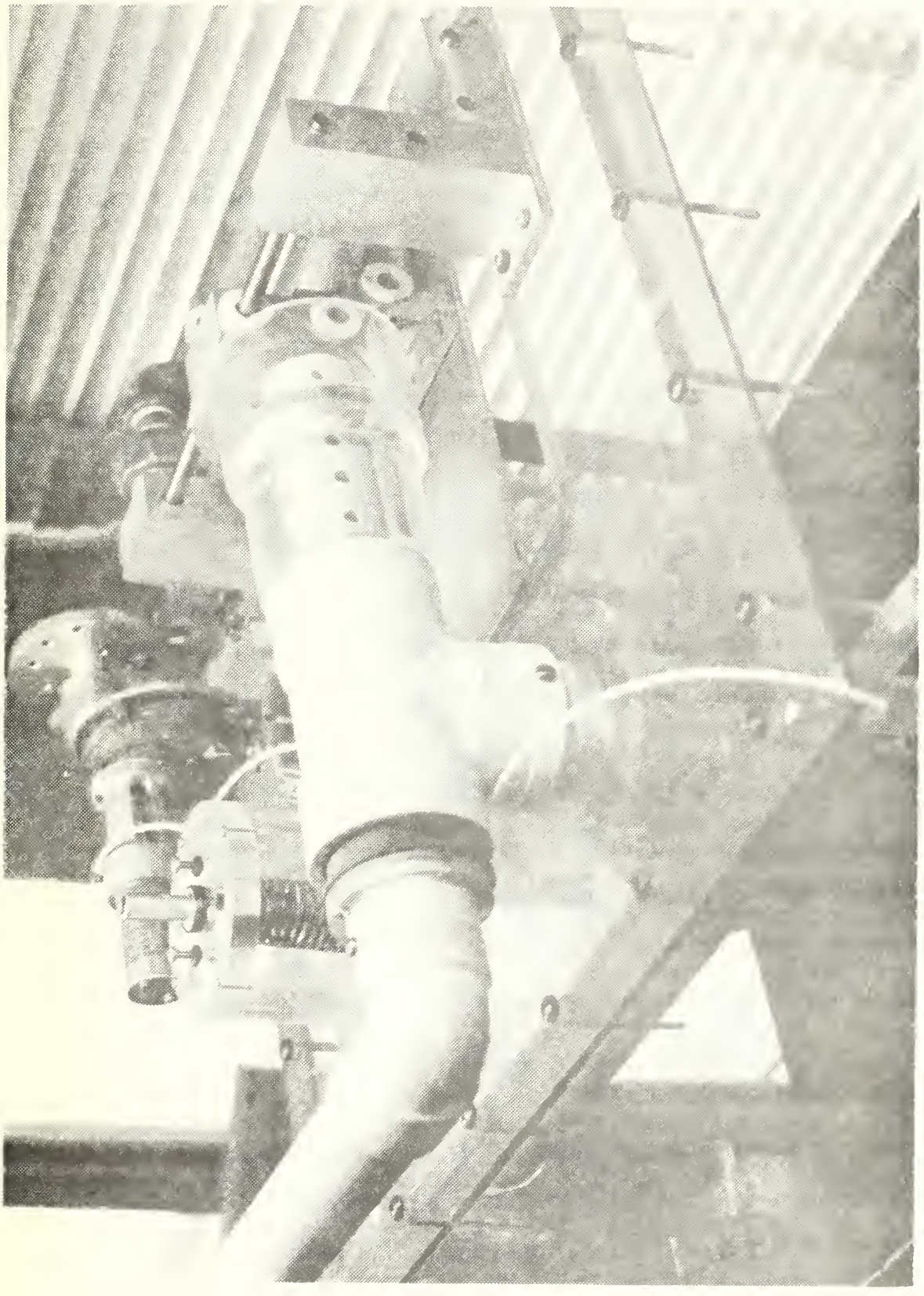

Figure 3. Oscillating mechanism.

The lateral and in-line force measuring devices consisted of various cantilever beams mounted to the outer surfaces of the test section. Eight piezoresistive strain gages were mounted on each cantilever beam and properly waterproofed. The drawing of one of the many such force transducers is shown in figure 4. The end of each beam firmly fitted into the self aligning bearings placed at each end of the cylinder.

These transducers were repeatedly calibrated by hanging loads at the mid section of the cylinders in the vertical and horizontal directions. Some of the force transducers were comprised of two pieces of thin cantilever beams cut orthogonal to each other. Thus they were capable of simultaneously measuring both the lateral and in-line forces. Some transducers were capable of measuring only the lateral or the in-line force. The one shown in figure 4 is of that type. It should be noted, however, that this particular transducer was rotatable ± 90 degrees. This enabled one to measure first the in-line force and then, after a 90 degree rotation, the lateral force. In all cases both the in-line and lateral forces were measured at both ends of the cylinder and compared with each other. In no case, did force curves deviate from each other, indicating a fairly uniform response along the cylinder as far as the resultant forces are concerned. The size of the cylinders varied from 1.0 inch to 2.5 inches. The spheres which were manufactured out of aluminum, or hard plastics with diameters ranging from

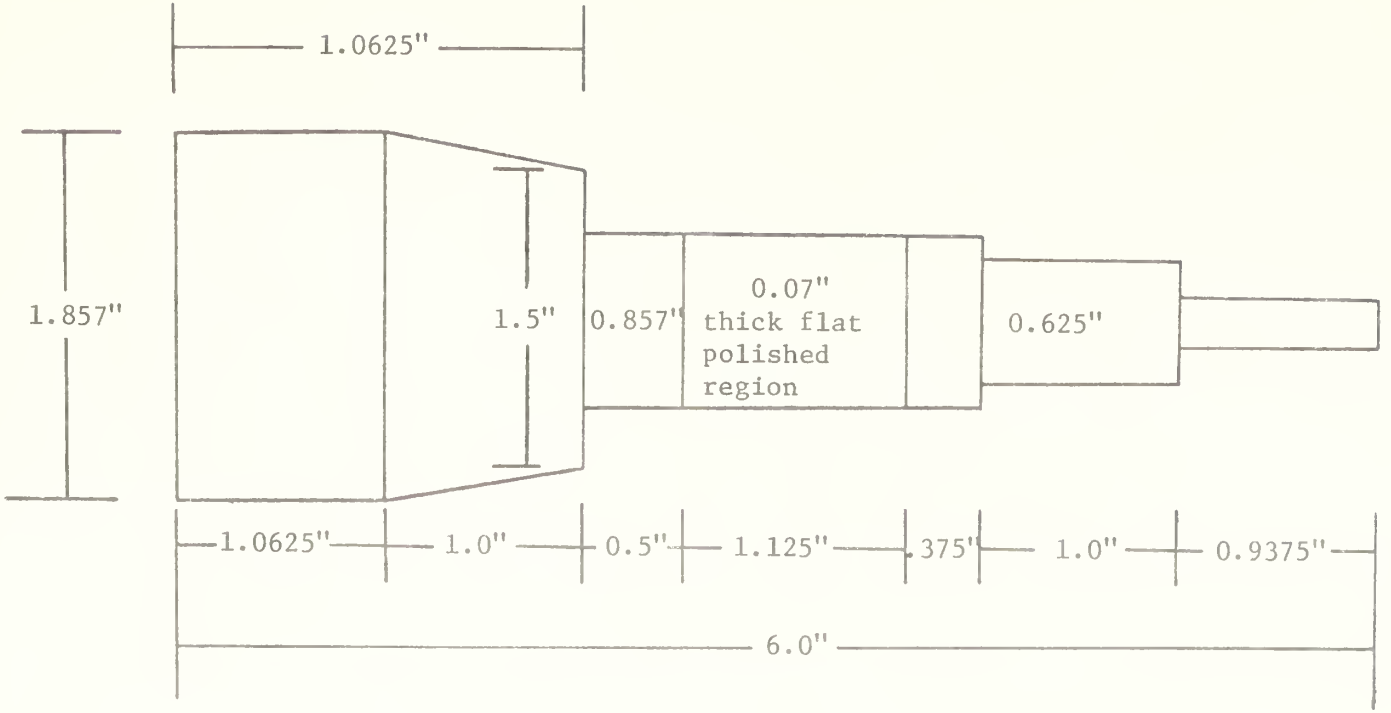

Figure 4. Dimensions of the force beam.

1.125 to 3.975 inches were hung with thin fish line from the force transducer placed at the top of the channel at the center of the test section. Attempts to prevent the spheres from swinging have resulted in the creation of undesirable oscillations in the force curves. Consequently, the spheres were allowed to hang freely and to respond to lateral forces. The amplitude of the swing naturally depended on the weight of the sphere. The maximum amplitude was approximately 0.25 inch. As noted earlier, the fish line was connected to another force transducer, similar to the one shown in figure 4, placed at the top of the channel.

Throughout the investigation the monitoring of the characteristics of the oscillations in the U-channel was of prime importance. As discussed in the introduction, most of the difficulties in the past in the determination of C_M, C_D, and C_{LMAX} resulted from the difficulty of creating a purely harmonic motion or from determining indirectly the characteristics of the oscillatory motion. Even though the U-channel has provided, by its very nature, a perfectly sinusoidal oscillation, both the instantaneous displacement and the acceleration were continuously monitored. The instantaneous elevation in one leg of the channel was determined through the use of a capacitance wire connected to an amplifier-recorder system. Such wires have been used in the past to measure wave heights in open channels. The response of the wire was found, through calibrations, to be perfectly linear within the range of oscillations encountered.

The instantaneous acceleration was measured by means of a differential-pressure transducer connected to two pressure taps placed vertically two feet apart at the mid-section of one of the walls of the U-channel. The instantaneous acceleration was then calculated from

$$\Delta P = \rho \ell a_z \tag{33}$$

where ΔP is the differential pressure, ρ the density of fluid, ℓ the distance between the pressure taps, and a_z the instantaneous acceleration of the fluid. The effect of the pressure drop due to the viscous forces over the length ℓ was found to be negligible.

Evidently, the displacement and acceleration traces are in phase and may be used independently to calculate the velocity and the displacement of the fluid. In fact such calculations have shown that the velocities and displacements calculated through the use of either traces did not differ more than 4%. Finally, it was gratifying to note that both the acceleration and displacement traces were nearly perfect sine curves. Figures 5, 6 and 7 show the representative displacement, acceleration, in-line force and lateral force traces for the cylinders and figures 8 and 9, the displacement, acceleration, and in-line force traces for spheres. These traces which were obtained without any damping of the disturbances show the smoothness of the variation of the various quantities and the degree of success achieved in obtaining a purely harmonic motion. It is also noted, from a brief perusal of the displacement and acceleration traces

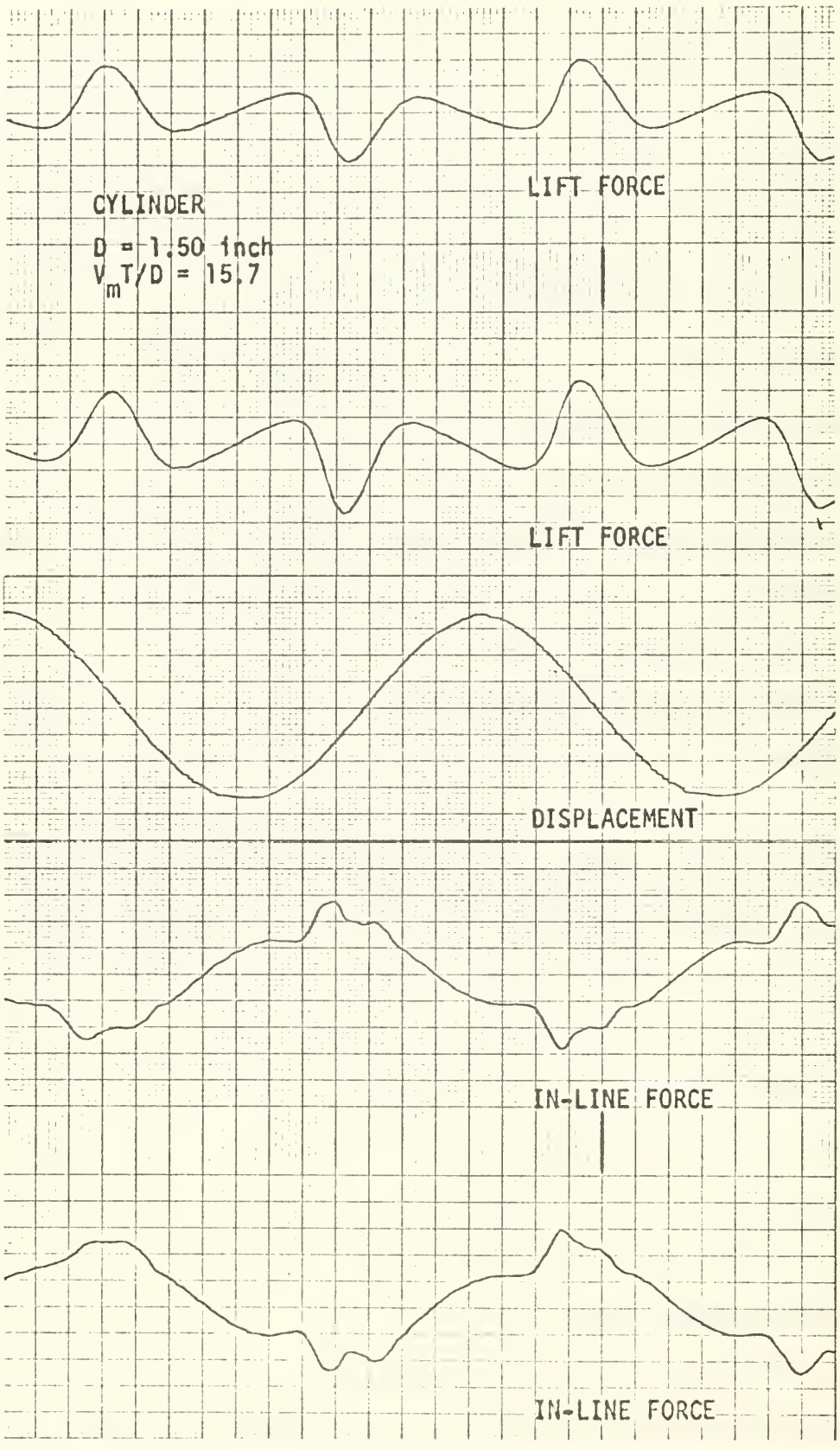

Figure 5. Force, displacement traces

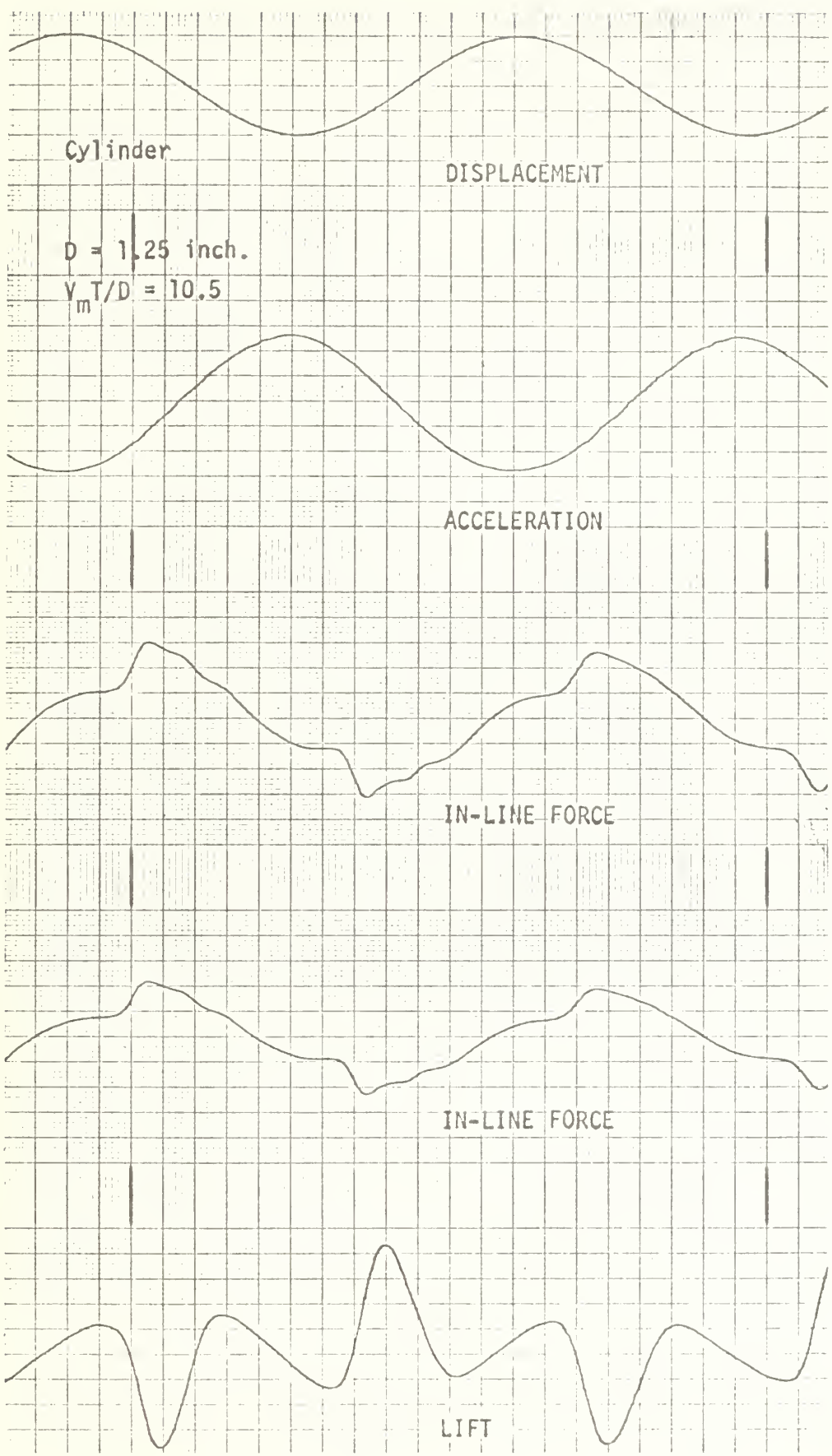

Figure 6. Force, displacement traces.

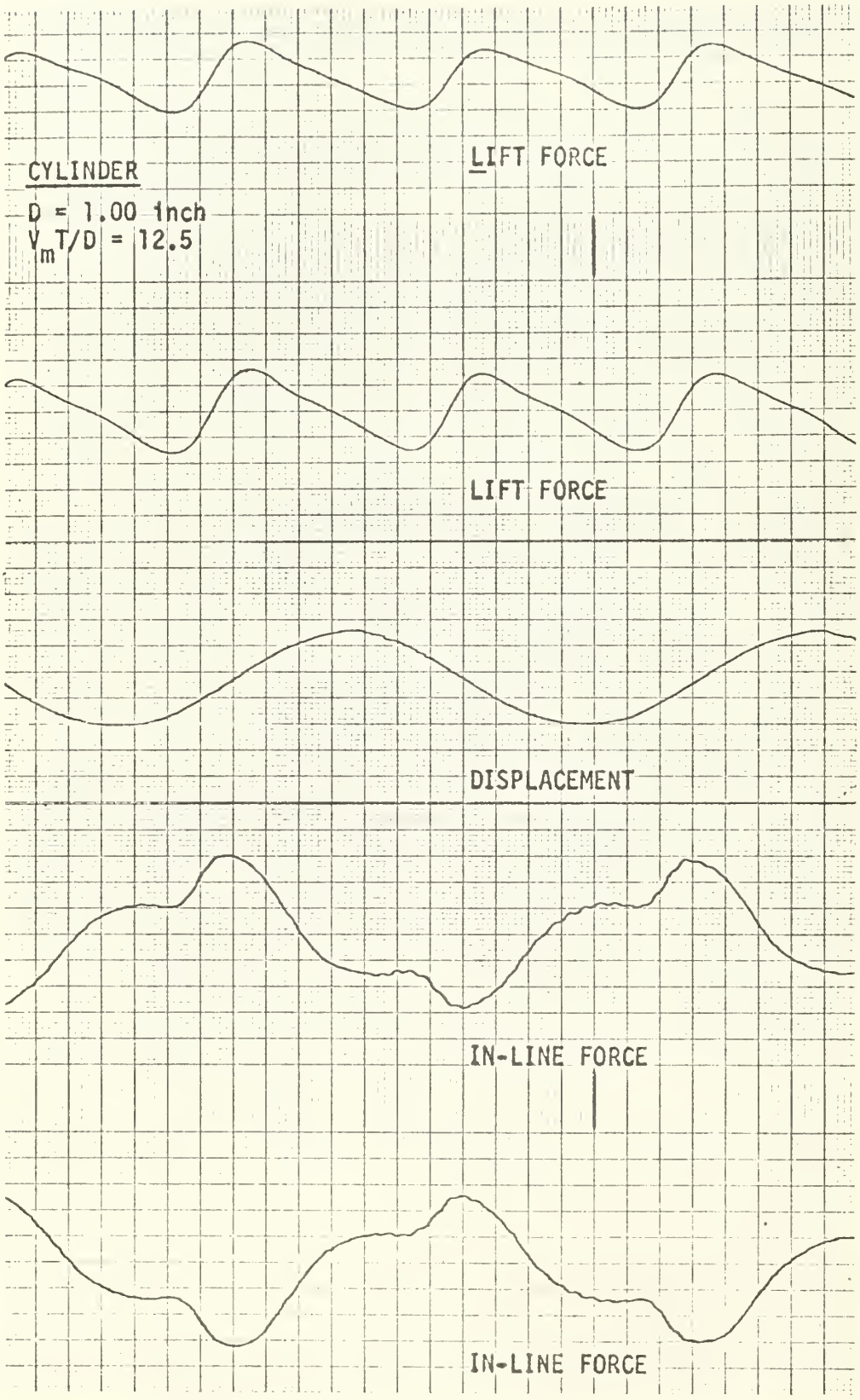

Figure 7. Force, displacement traces.

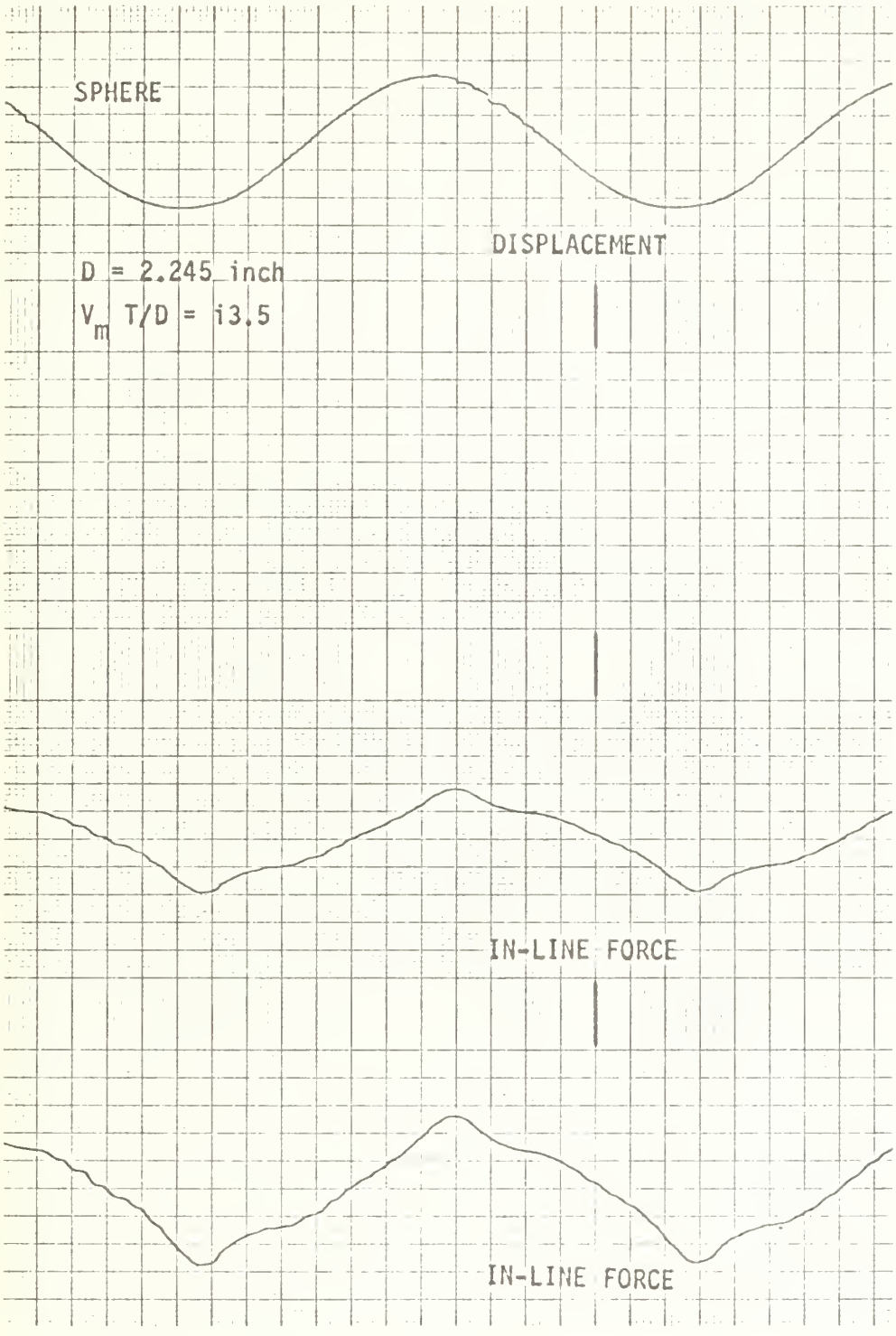

Figure 8. Force, displacement traces.

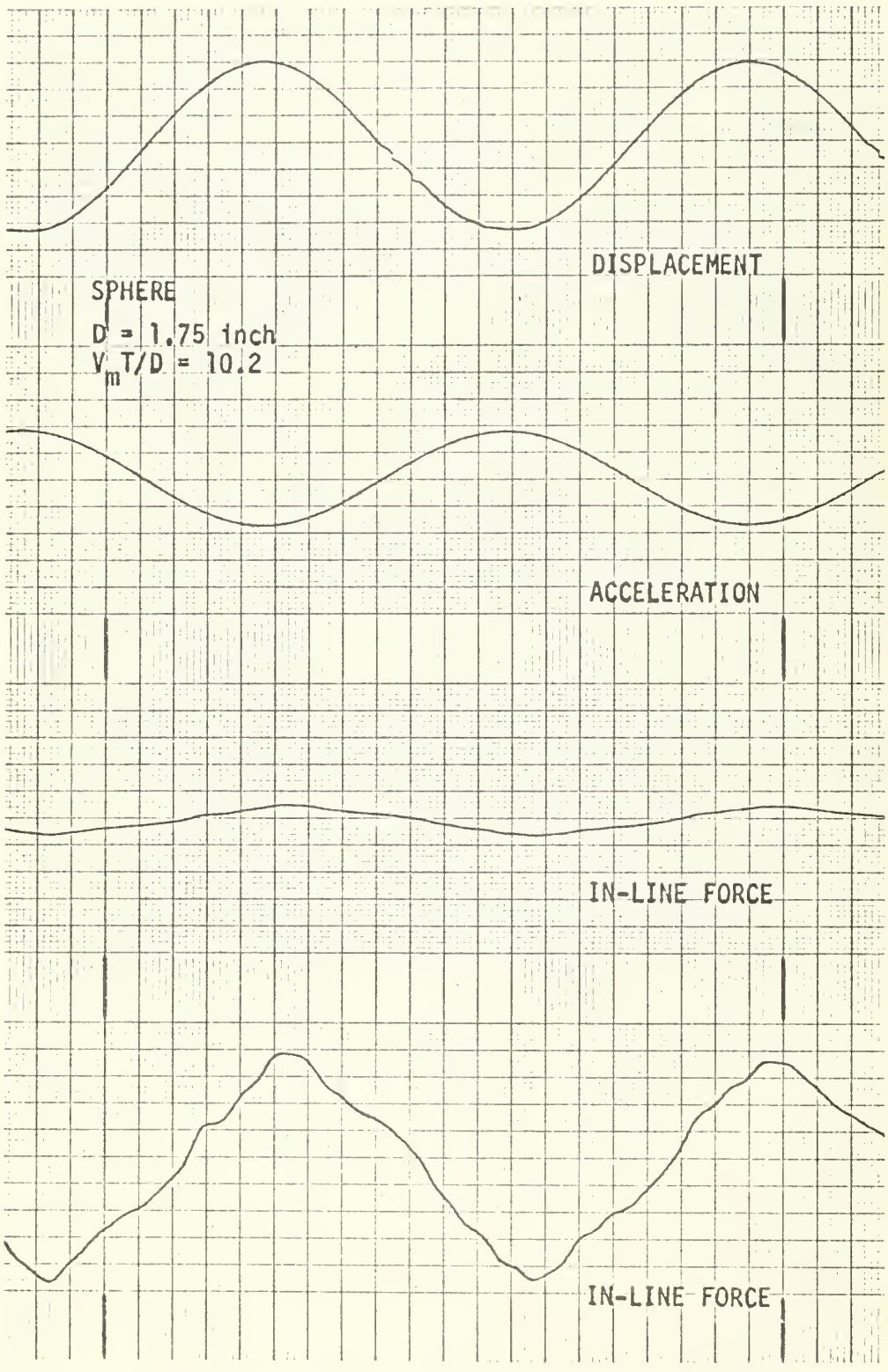

Figure 9. Force, displacement traces.

that the damping of the oscillations over a cycle is imperceptibly small when the fluid is let to freely oscillate in the channel.

B. PROCEDURE

From the traces similar to those described above, the amplitude of oscillation and the maximum velocity were calculated. Then the in-line force from the force traces was read and punched on cards for every 2.5 mm (this corresponded to $\Delta t/T = 0.039645$ for the period of $T = 2.86$ seconds). Then the drag and inertia coefficients were calculated through the computer programs given in Appendix A. This part of the procedure was identical for both cylinders and spheres.

The calculation of the maximum lift coefficient consisted of the determination of the maximum amplitude of "lift" or lateral force for a given $V_m T/d$ through the use of equation (32).

It was realized before the start of investigation that not only the magnitude but also the frequency of the oscillations of the lateral force is of major importance as far as the design of bodies subjected to harmonic fluid motions is concerned. With this idea in mind, the frequency or frequencies occurring in lateral forces in each cycle were determined for each $V_m T/d$.

The maximum lift force in each cycle was also compared with the maximum value of the in-line force, as will be discussed later.

Finally the phase angle between the occurrence of the maximum force and the maximum velocity was determined from the recorder traces for both the cylinder and sphere.

IV. DISCUSSION OF RESULTS

A. CYLINDER DATA

The primary purpose of this investigation was the determination of the forces exerted on cylinders and spheres in harmonically oscillating fluids. The secondary purposes were the re-examination of the data obtained by Keulegan and Carpenter [Ref. 18] and, whenever possible, the evaluation of the secondary effects such as non-harmonic oscillations, viscous forces, etc. on the forces obtained with harmonic oscillations.

The drag and inertia coefficients for cylinders are shown in figures 10 and 11 as a function of the period parameter V_mT/d. The data follow in general the same trend of that obtained by Keulegan and Carpenter for very small values of V_mT/d, C_M is equal to about 2.0 and C_D is nearly zero. For V_mT/d equal to about 11.0, C_D reaches its maximum value of about 2.1 and C_M reaches its minimum value of about 0.8. Considering the fact that $C_M = 1.0+k$ where k is the added mass coefficient, it is apparent that for some values of V_mT/d the added mass coefficient may become negative. A similar result has also been obtained by Keulegan and Carpenter. For larger values of V_mT/d, C_M is nearly equal to 1.2 and C_D approaches 1.4, within the range of V_mT/d values encountered in the present investigation.

Mean lines have been passed through the data shown in figures 12 and 13 and these mean values are compared in

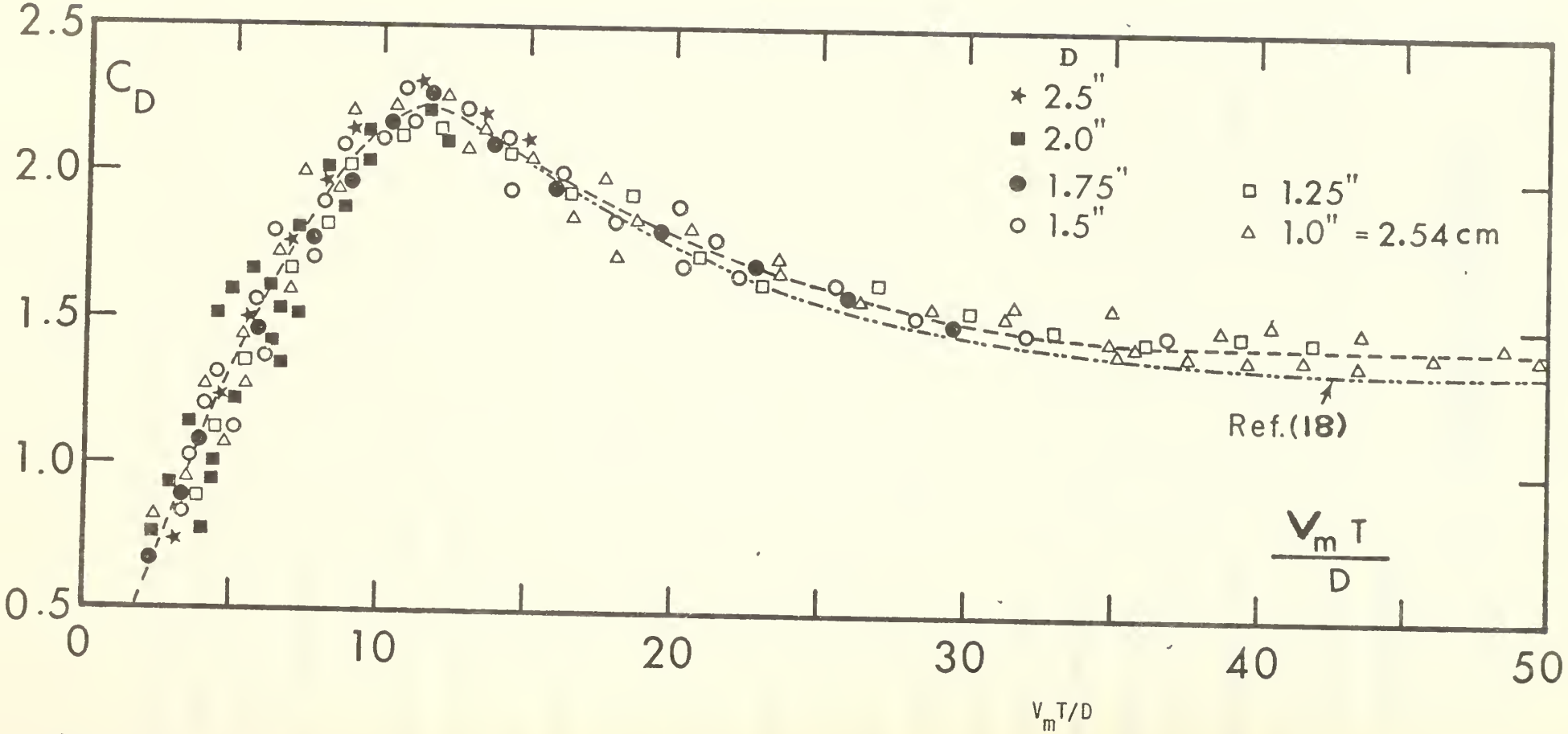

Figure 10 C_D versus the period parameter for cylinders

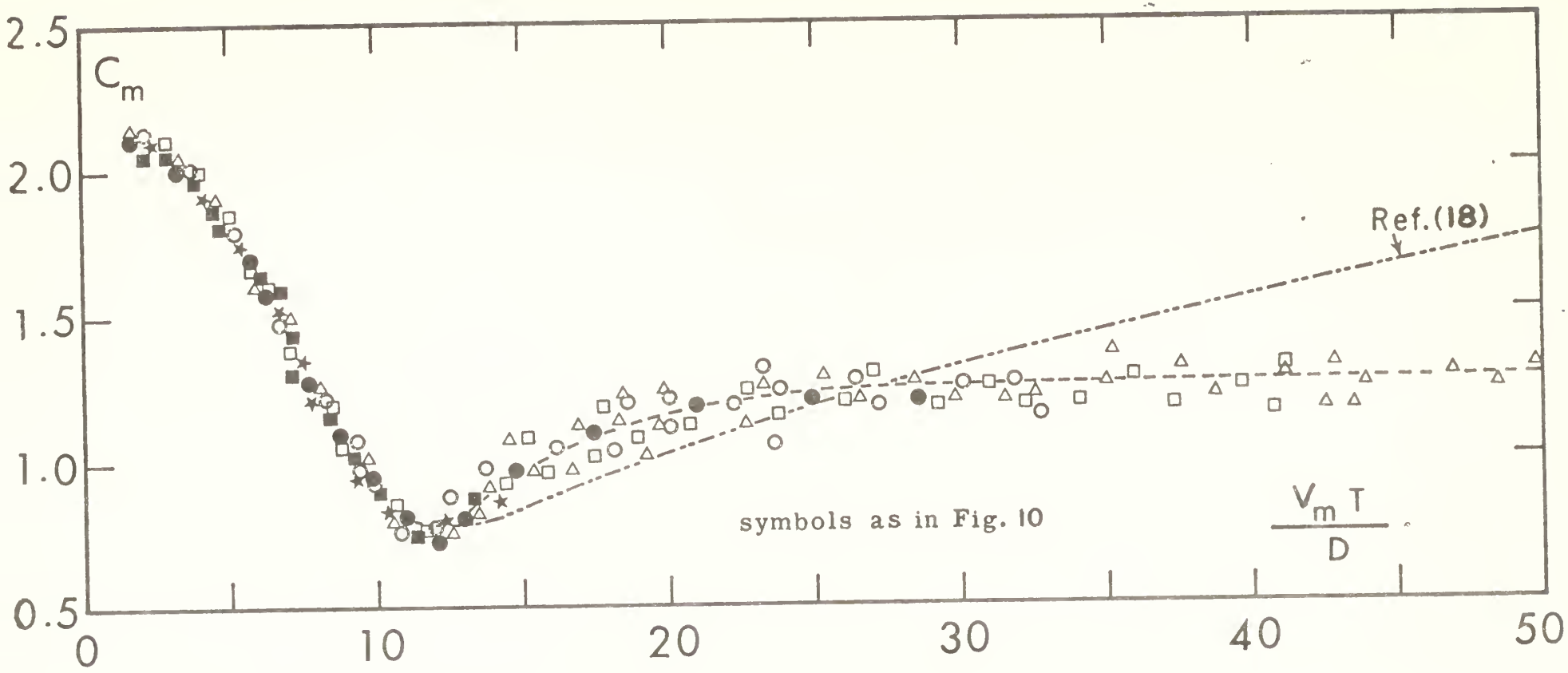

Figure 11 C_M versus the period parameter for cylinders

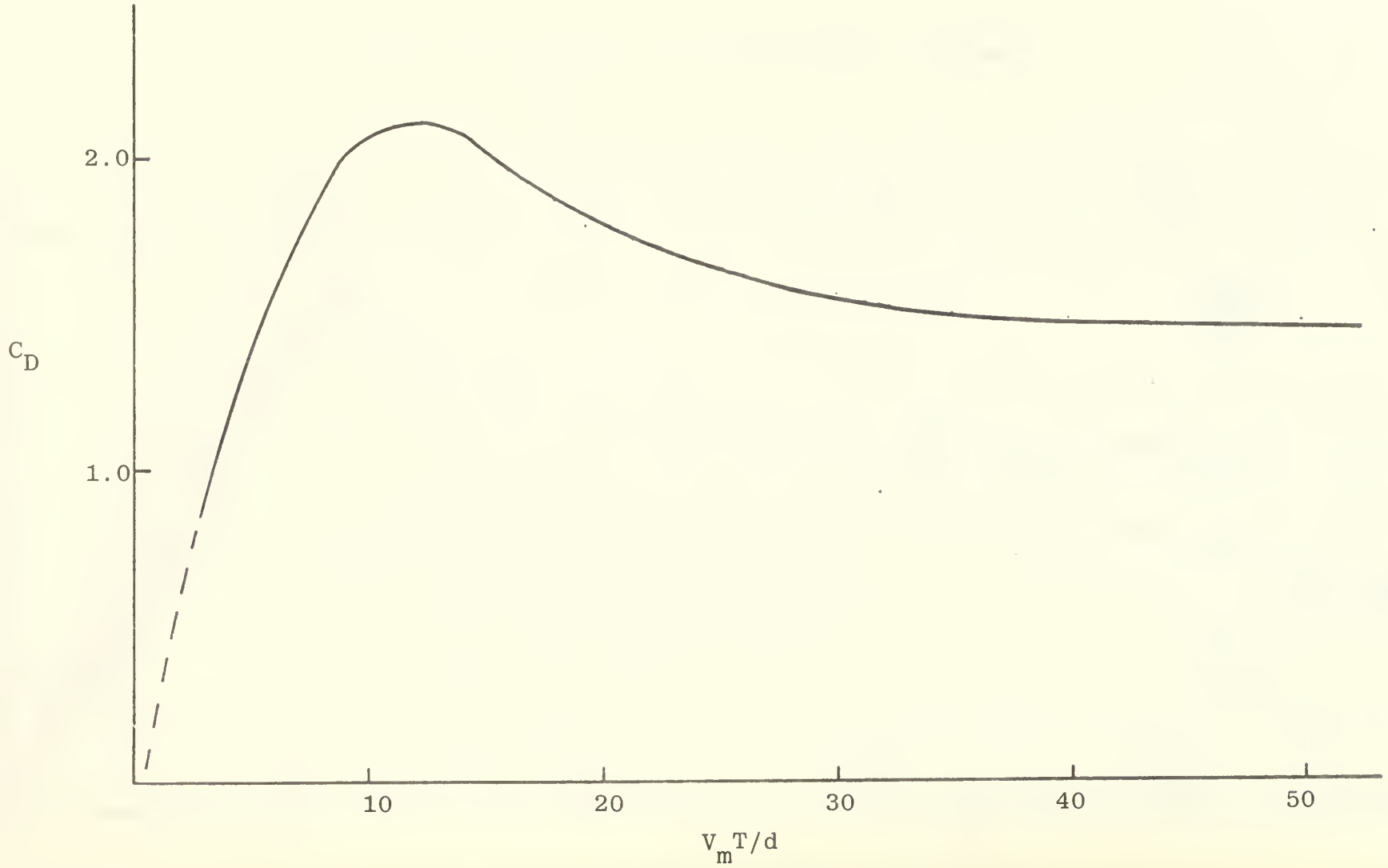

Figure 12. Mean line of C_D for cylinders.

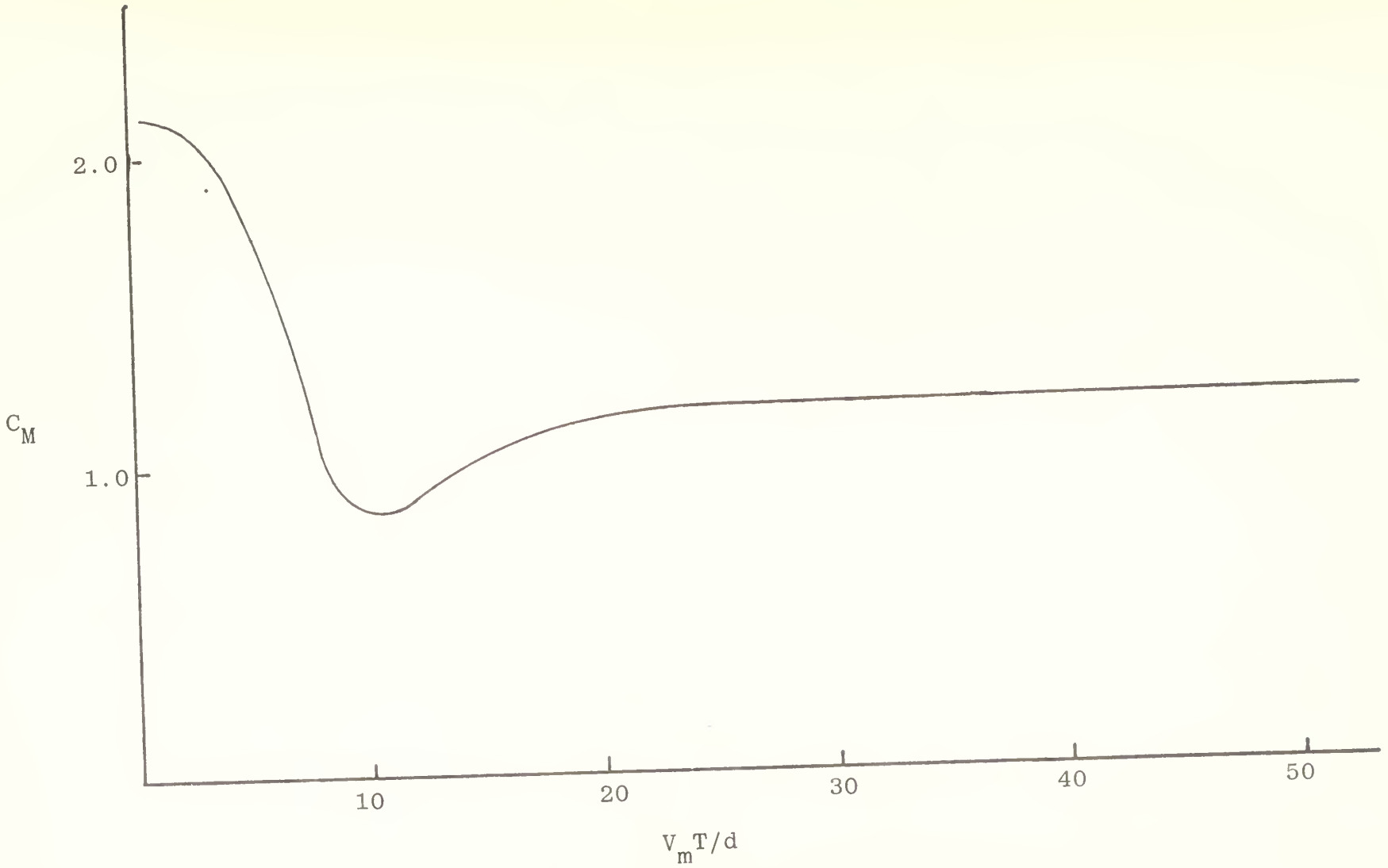

Figure 13. Mean line of C_M for cylinders.

figures 14 and 15 with the corresponding mean lines obtained by Keulegan and Carpenter. Evidently, for smaller values of $V_m T/d$ the results of the two independent studies are comparable. For larger values of $V_m T/d$, however, the Keulegan and Carpenter study shows relatively larger values for C_M. Even though it is not easy to explain the difference, it may be conjectured that the relatively few data points obtained by Keulegan and Carpenter through the use of a 0.5 inch diameter cylinder may have been in error or the standing waves corresponding to the large values of $V_m T/d$ may not have followed the particular analysis used in the prediction of their characteristics. Furthermore, in this range of $V_m T/d$ values, the inertial force is small relative to the drag force. This in turn leads to an unstable determinant in the equations yielding C_M and C_D.

It has been conjectured first by McNown and Keulegan [Ref. 21] and later by Sarpkaya and Garrison [Ref. 27] that there should be a unique relationship between C_M and C_D if each of these coefficients are dependent only on $V_m T/d$. To explore this matter further, a plot has been prepared as shown in figure 16. The numbers on this figure give the corresponding $V_m T/d$ values. Even though of no particular practical significance, the variation of C_M with C_D is indicative of the existence of a complex relationship between the two coefficients. The data points are a step further removed from the actual fluid motion through the elimination of $V_m T/d$. Thus, such a plot may be of some significance if

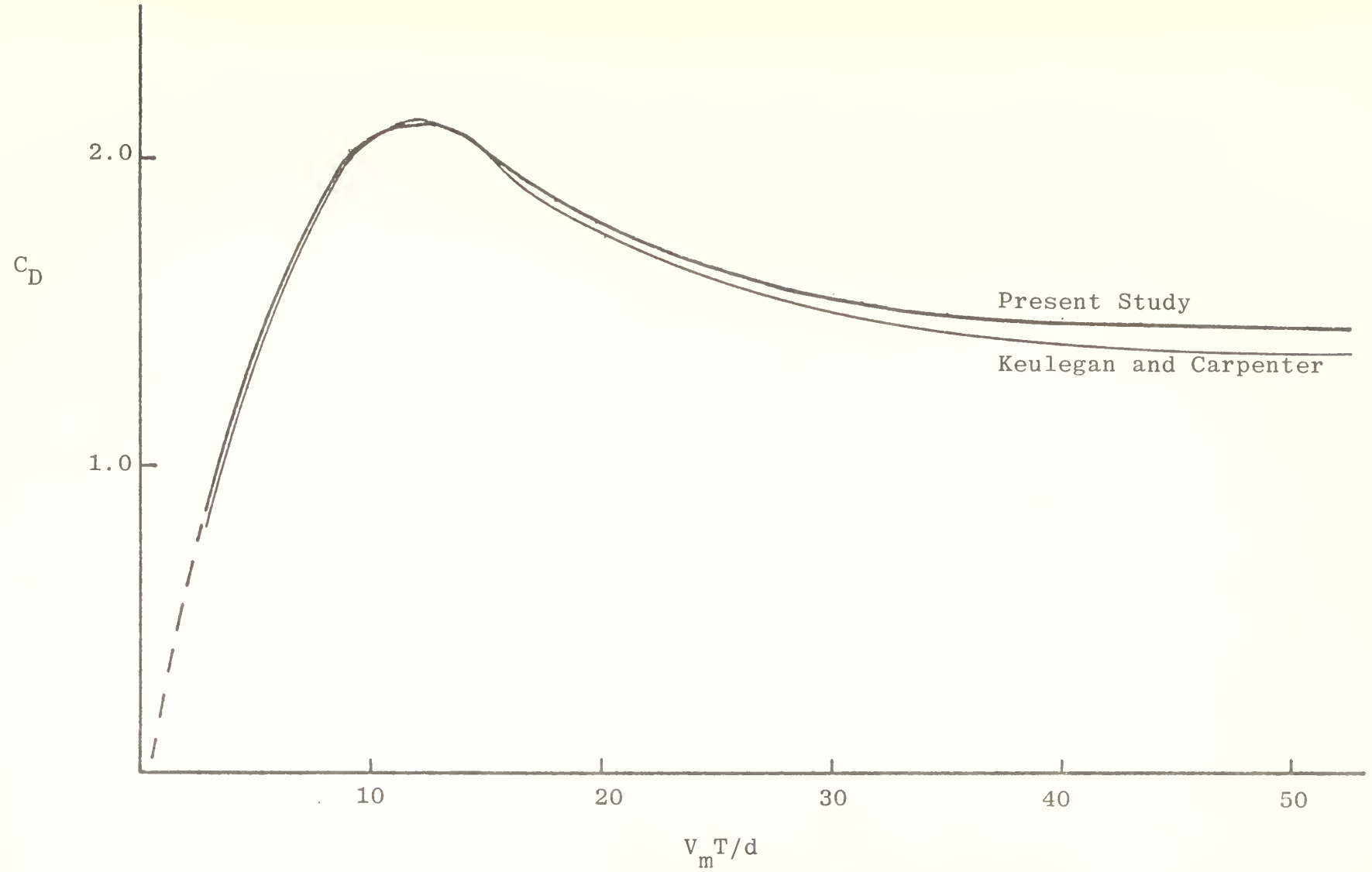

Figure 14. Comparison of C_D with Keulegan and Carpenter data.

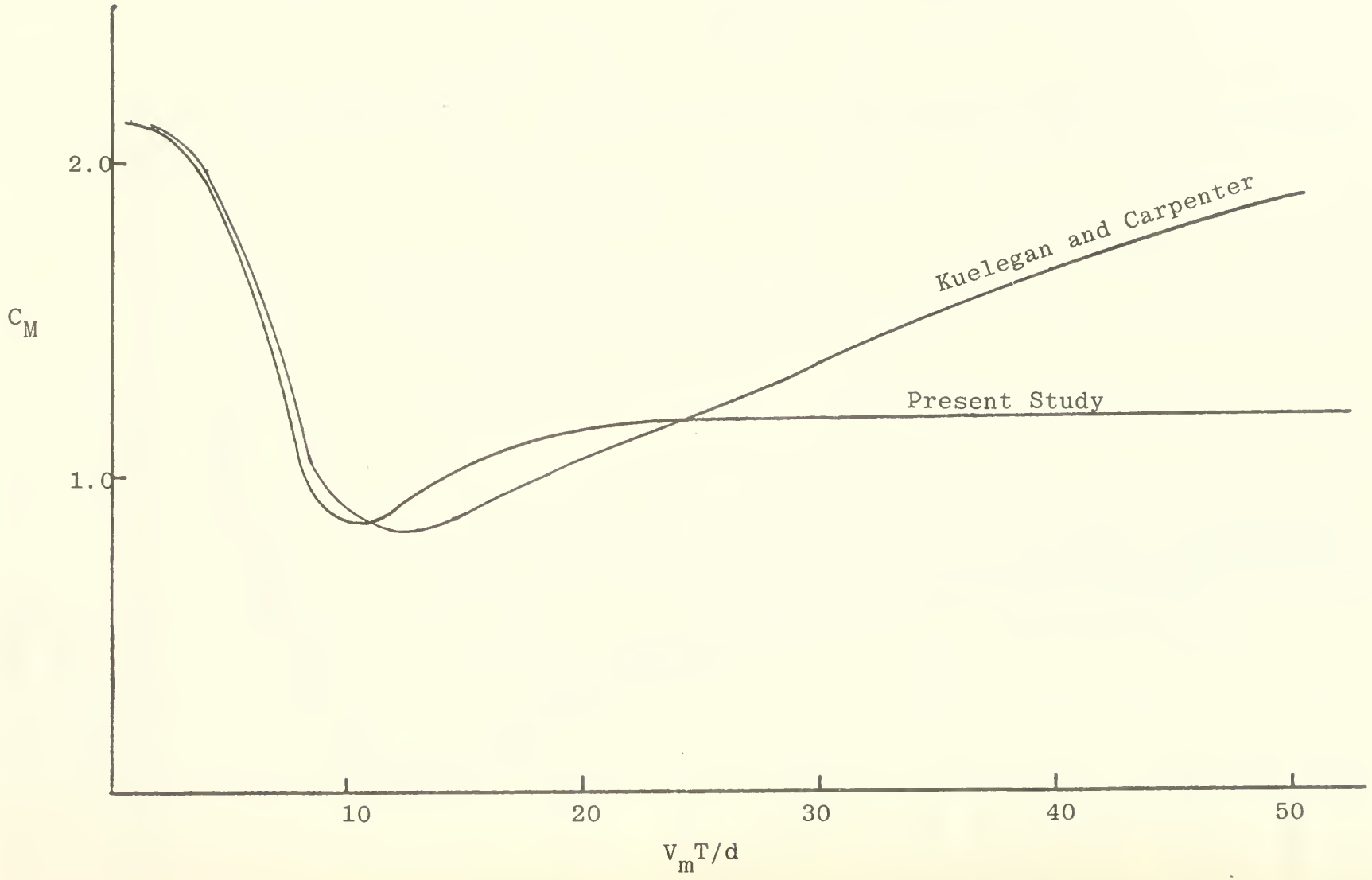

Figure 15. Comparison of C_M with Keulegan and Carpenter data.

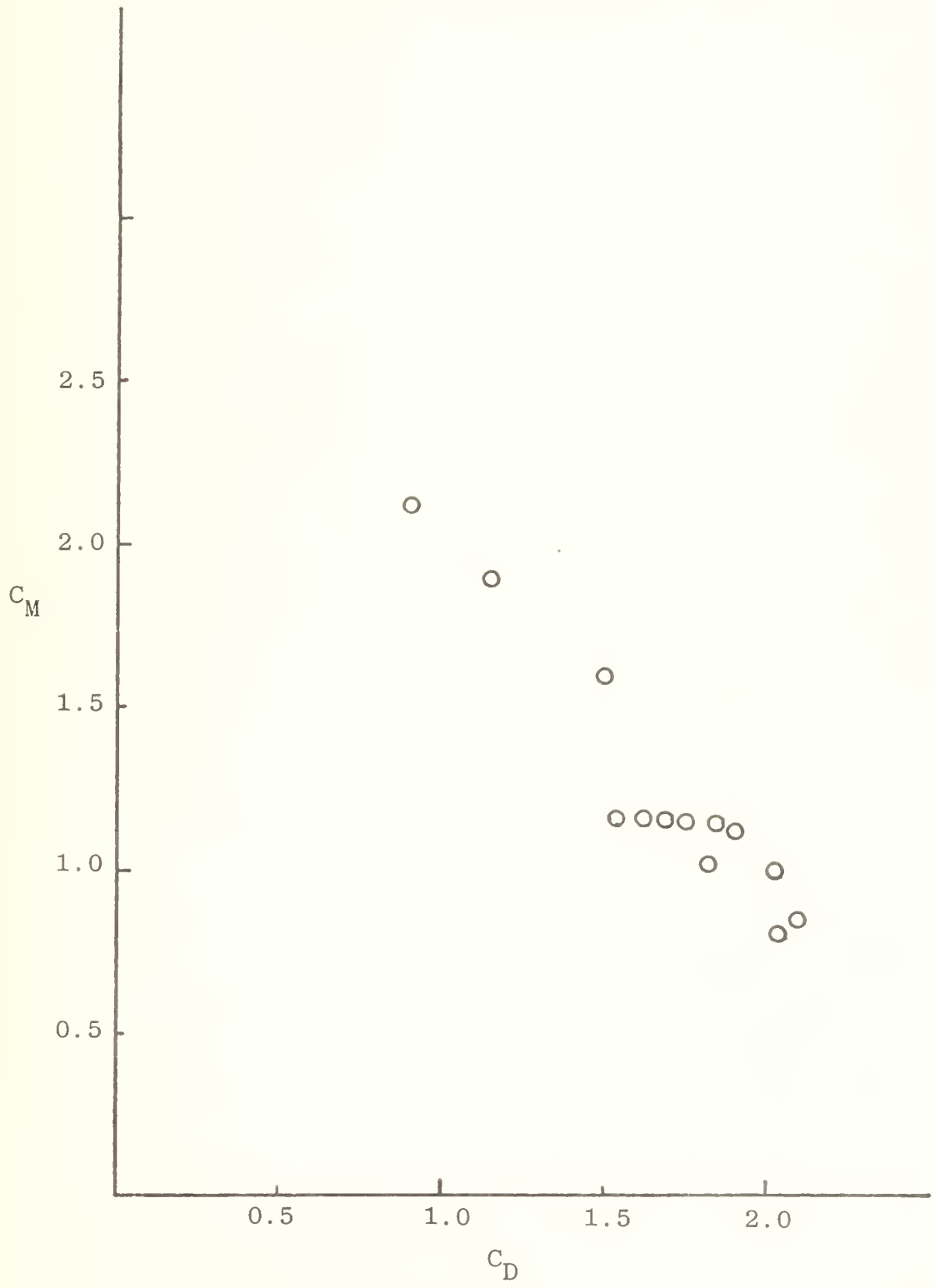

Figure 16. C_M versus C_D for cylinders.

and when the problem could be analyzed numerically or otherwise.

The phase angle between the occurrence of maximum in-line force and maximum velocity which is also a measure of the ratio of the relative magnitudes of the inertia and drag forces, is evaluated from the traces and is shown in figure 17. Evidently for V_mT/d values less than about 8 or 10 there is a large phase difference between the occurrence of the maximum force and the maximum velocity. In this range, the maximum velocity leads the maximum force. For V_mT/d values larger than about 20, there is a very small phase difference between the two quantities cited. For very large values of V_mT/d, the phase angle drops nearly to zero. It may thus be concluded that the inertial forces dominate the motion for V_mT/d values less than about 8. For larger values of V_mT/d, the drag force is dominant. Thus for structures subjected to wave forces with V_mT/d values less than about 8, the drag forces may be ignored. The alternate is true for V_mT/d larger than about 10.

The maximum lift coefficient, defined by equation (32), is shown in figure 18 again as a function of V_mT/d. Such data, which are presented herein for the first time, have several significant features. Firstly, the maximum lift coefficient may reach a value as high as 3.0. Secondly the lift coefficient has several maxima and minima dependent on V_mT/d. The lift traces show that the lift force does not begin to develop for V_mT/d less than about 4.0. Then the

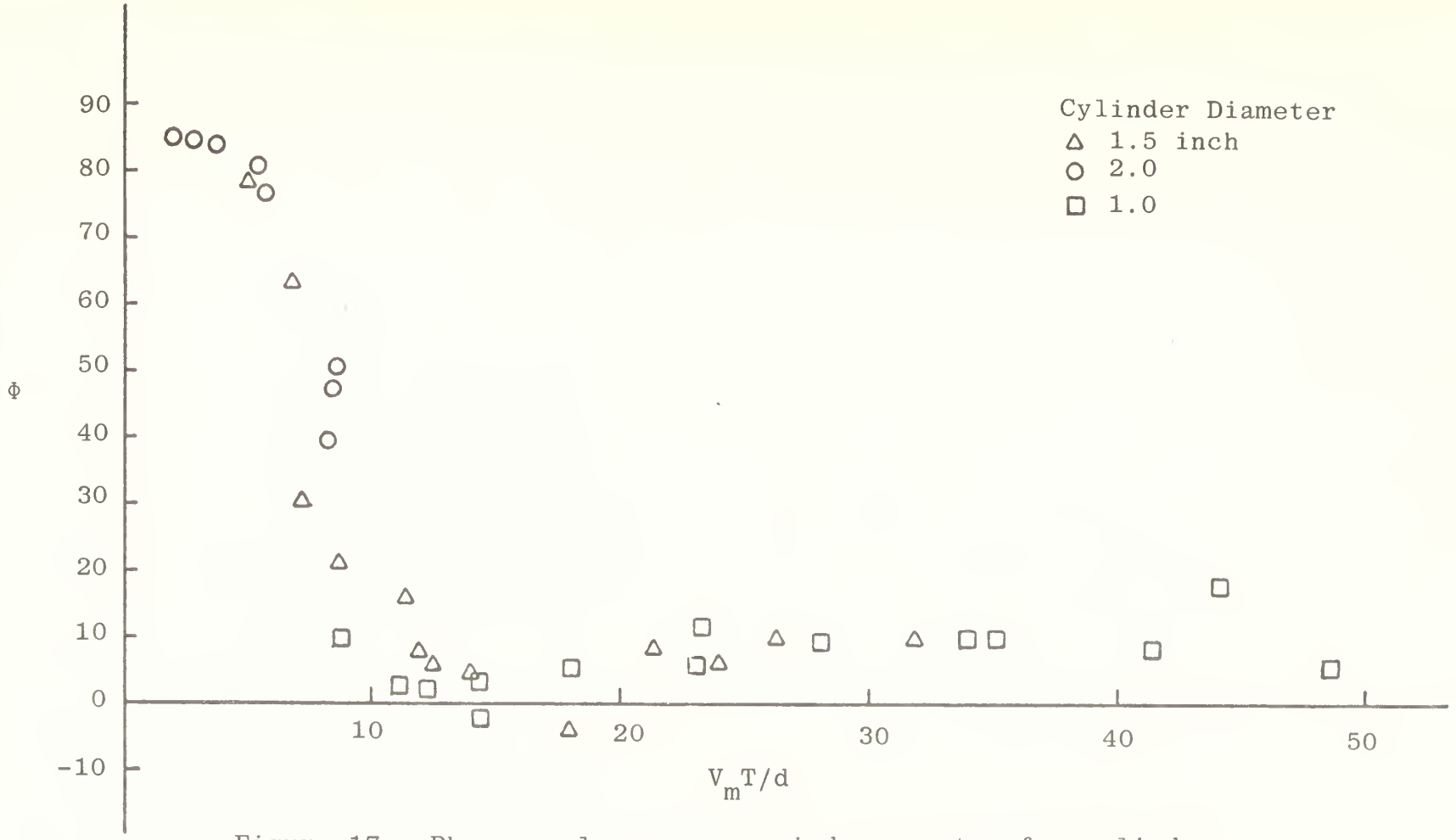

Figure 17. Phase angle versus period parameter for cylinders.

lift coefficient increases rapidly reaching its first maximum value of about 2.85 at $V_mT/d \simeq 10.0$. The significance of the existence of large lift forces between $10 > V_mT/d > 4$ lies in the fact that even when the forces in line with the fluid motion are essentially of inertial nature ($V_mT/d < 8$), there is still a region, ($4 < V_mT/d < 8$) in which considerable lateral forces may act upon the cylinder. Thus, if one were to ignore separation and vortex shedding and determine through the use of inviscid fluid flow analysis the forces acting on the cylinders, the results should not be extrapolated beyond $V_mT/d > 4$.

The lift coefficient sharply decreases in the range $10 < V_mT/d < 15$ and then increases again to a value of about 3.0. Subsequently, C_{LMAX} gradually decreases to about unity. It is apparent from the data shown in figure 18 that there is considerable scatter in the range of V_mT/d from about 18 to 25. The reasons neither for this scatter nor for the rapid drop and rise for V_mT/d from 10 to 18 can be explained in simple terms. They can, however, be attributed to the complex interaction of the shed vortices aft and fore of the cylinder and to the fact that we have not decomposed the lift force into its harmonics.

Several attempts have been made to visualize the flow with various dyes and particles and to obtain motion pictures. These efforts were only partially successful in identifying the instantaneous positions of the vortices. Efforts were also made to visualize the flow pattern in a water

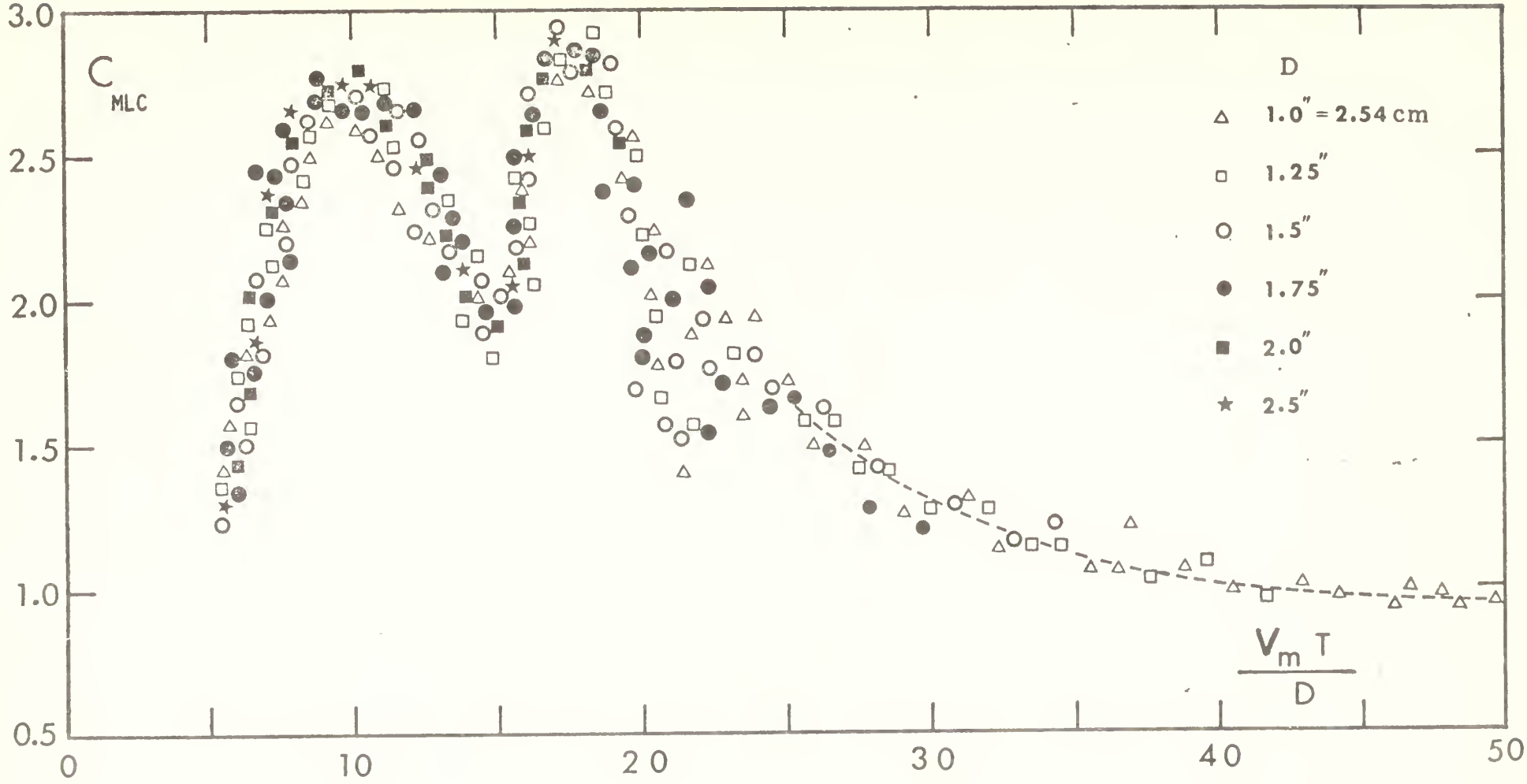

Figure 18 Maximum-Lift Coefficient versus the period parameter

table with a free surface. The strong effects of the surface tension have prevented the identification of the vortices. At small values of $V_m T/d$ beautiful patterns of acoustic streaming have been observed.

As cited in the development of the so-called Morison's equation, the coefficients C_M and C_D are Fourier averaged and thus assumed constant over a cycle. In reality, the unsteady nature of the flow renders these coefficients time dependent and thus gives rise to some differences between the measured and calculated forces. This difference, called error or remainder force, could be estimated either through the use of the additional terms appearing in equation (11) or through the evaluation of the percent difference between the measured and calculated forces. The former technique which was used by Keulegan and Carpenter [Ref. 18] may still differ from the actual error between the measured and calculated forces. With this view in mind it was preferred to calculate the actual error in each cycle for representative values of $V_m T/d$ as well as the error corresponding only to the maximum force for all values of $V_m T/d$. For this purpose the percent error was written as

$$\lambda = \frac{F_{mes} - F_{cal}}{(F_{mes})_{max}} \tag{34}$$

and

$$\lambda^* = \frac{F_{mes(max)} - F_{cal(max)}}{F_{mes(max)}} \tag{35}$$

The values of λ for representative values of V_mT/d are presented in Appendix B. The variation of λ^* with V_mT/d is shown in figure 19. Evidently the maximum value of λ^* occurs at $V_mT/d \simeq 12$ and is in the order of 15%. Thus, the designer must multiply the calculated values with λ^* in determining the maximum actual force acting on the cylinders.

So far attention has been paid to the calculation of the lift, drag, and inertia forces and nothing has been said either on the frequency of the lateral or lift forces or on the ratio of the maximum lift force to the maximum in-line force.

As cited earlier, the frequencies of lateral forces in each cycle for each V_mT/d have been evaluated for all cylinders tested and plotted in figure 20. Such a plot which has never been presented in the literature before, shows several interesting features. Firstly the vortex shedding frequency is not a constant fraction of the oscillation frequency ($f = 1/T$) and that several frequencies may occur during a given cycle. This may appear to be a priori evident considering the fact that in an oscillating flow the instantaneous velocity of fluid varies from zero to V_m and that there cannot be a single Strouhal frequency. Secondly, there does not seem to be any lateral force for V_mT/d less than about 4.0. Considering the fact that V_mT/d may also be regarded as a measure of the relative displacement of a fluid particle, for small relative displacements vortices are shed at two distinct frequencies: one at the oscillating flow frequency,

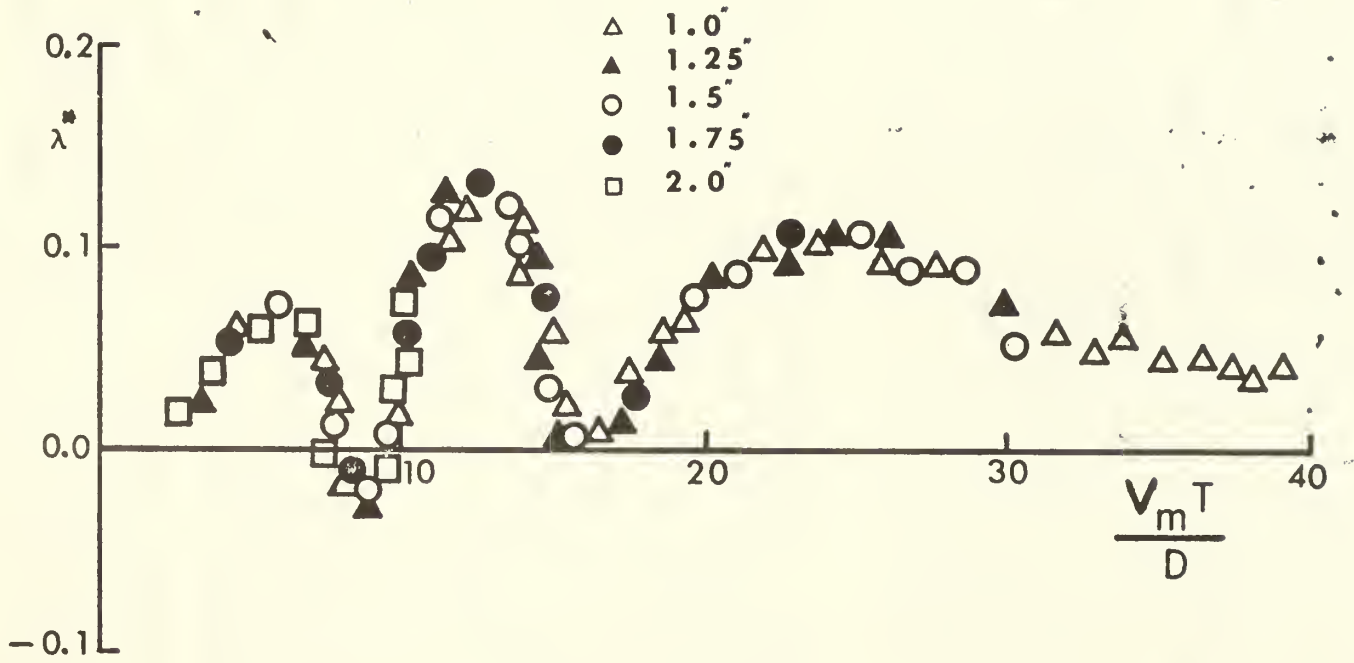

Figure 19 Error based on maximum force versus the period parameter

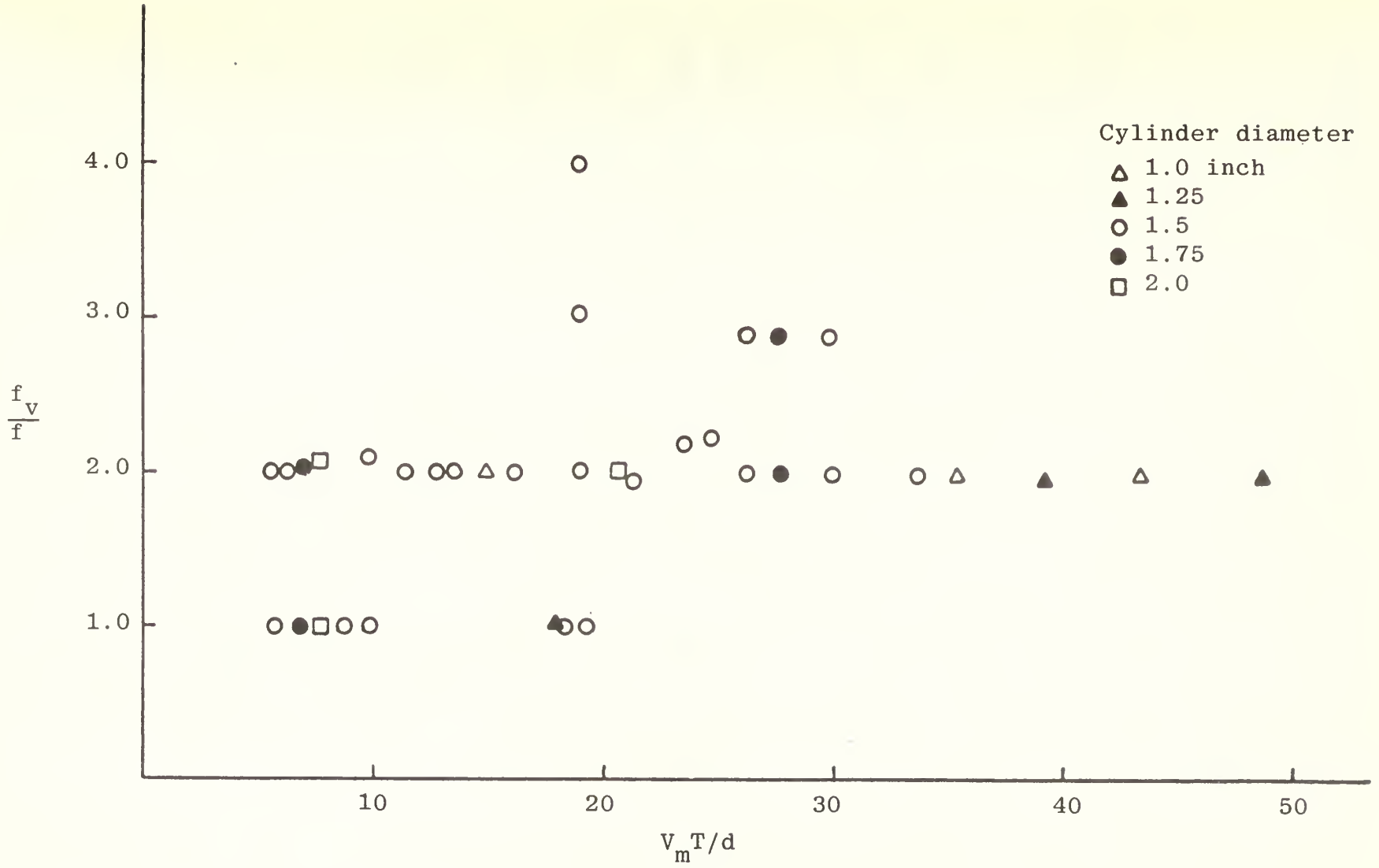

Figure 20. Lift frequency versus period parameter.

i.e. f, and the other at 2f. For some values of $V_m T/d$, the vortices may be shed at as many as three or four different frequencies, namely, at f_v = f, 2f, 4f, etc. For $V_m T/d$ larger than about 35 the vortex shedding frequency is limited to a single frequency of 2f.

The significance of the existence of multiple frequencies in periodic flows stems from the fact that a structure may, under certain circumstances, come into resonance with the frequency of the exciting lateral forces acting on it. For waves of large periods this frequency may be sufficiently small to match the natural frequency of highly elastic thin members. It is not expected that highly stiff and large cylindrical structures would be excited by long waves. Thus a cylindrical pile may go into resonant motion at relatively smaller wave periods at or near the frequencies twice the frequency of waves. The subject of vortex-synchronization will not be discussed here further since the cylinders were held almost rigidly at rest in the pulsating flow.

As to the magnitude of the lateral force relative to the maximum in-line force, a plot has been prepared representing this ratio in terms of $V_m T/d$. The purpose of this effort was to emphasize the fact that the lateral forces could, under certain circumstances, be considerably larger than the in-line forces. In fact in the range $5 < V_m T/d < 15$, the said ratio is as large as 1.5. Thus in calculating the maximum total force acting on the cylinder one must consider the vectorial sum of the lateral and in-line forces. With

this view in mind a total force coefficient defined by

$$C_T = \frac{\sqrt{F^2_{D(max)} + F^2_{L(max)}}}{\frac{1}{2}\rho U_m^2 d\ell} \tag{36}$$

was calculated for two representative cylinders and the results were plotted in figure 21. Evidently, C_T may reach values as high as 4.0 in the vicinity of $V_mT/d \simeq 10$. It should be noted that the total force coefficient calculated in this manner is somewhat larger than the actual total force coefficient since the maximum lift force does not necessarily occur at the same instant as the maximum in-line force. However, considering the complexity of the lift force and the possibility of the simultaneous occurrence of the maximums of the two forces it was preferred to calculate the total force coefficient as given above. No attempt was made to analyze in detail the phase angle between the first and higher harmonics of the lift force and the maximum in-line force. A perusal of the data has shown that there are many instances where the two forces occur almost simultaneously. It is evident from the foregoing discussion that what is most important for the design of structures in such flows is not the drag and inertia coefficients for the in-line force but rather a total force coefficient which fully accounts for both the in-line and the transverse forces.

The dependence of C_M and C_D on the Reynolds number was investigated by plotting both coefficients as a function of Reynolds number for various values of V_mT/d. As seen from figures 22 and 23 neither of the two coefficients depend

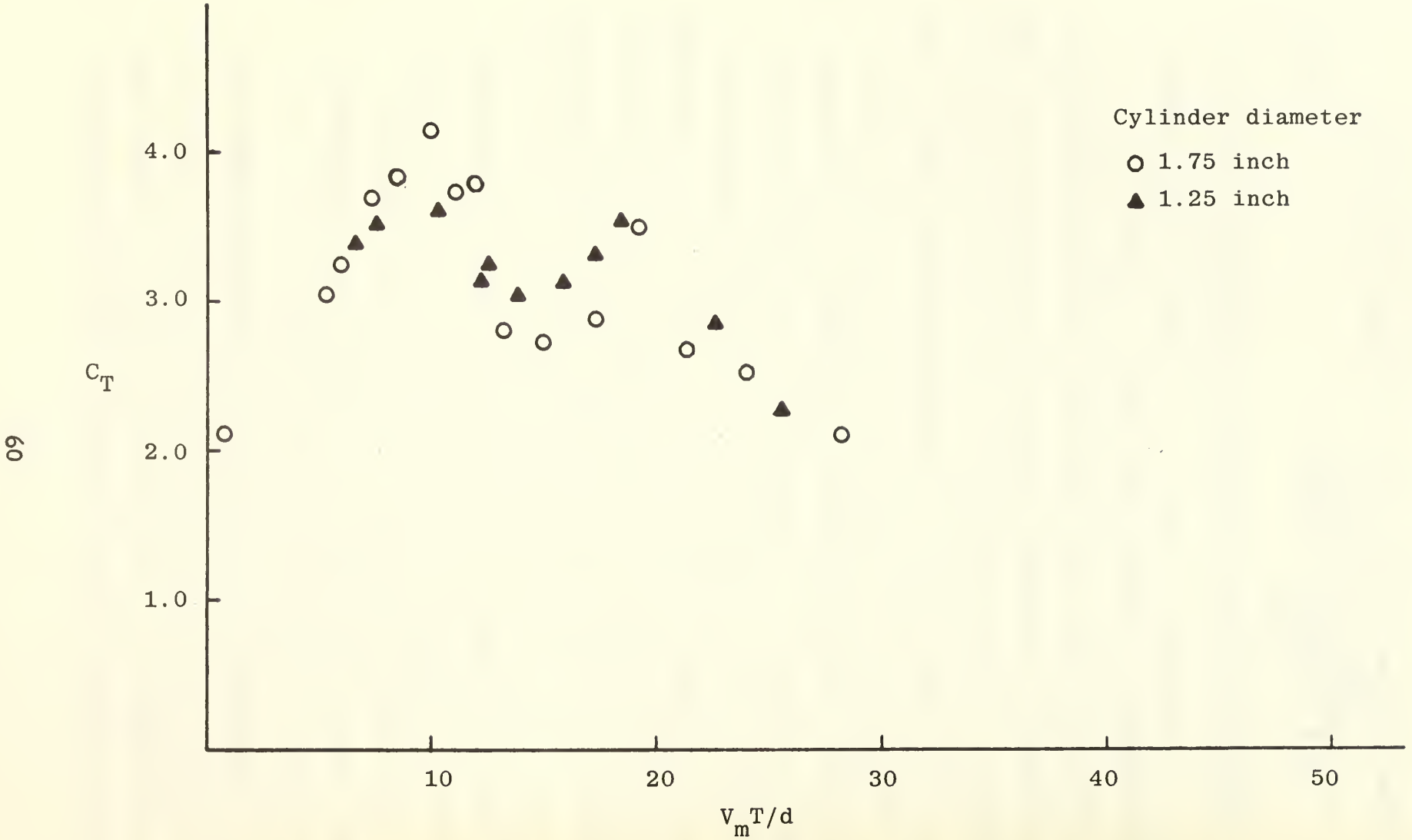

Figure 21. Maximum total force coefficient versus period parameter.

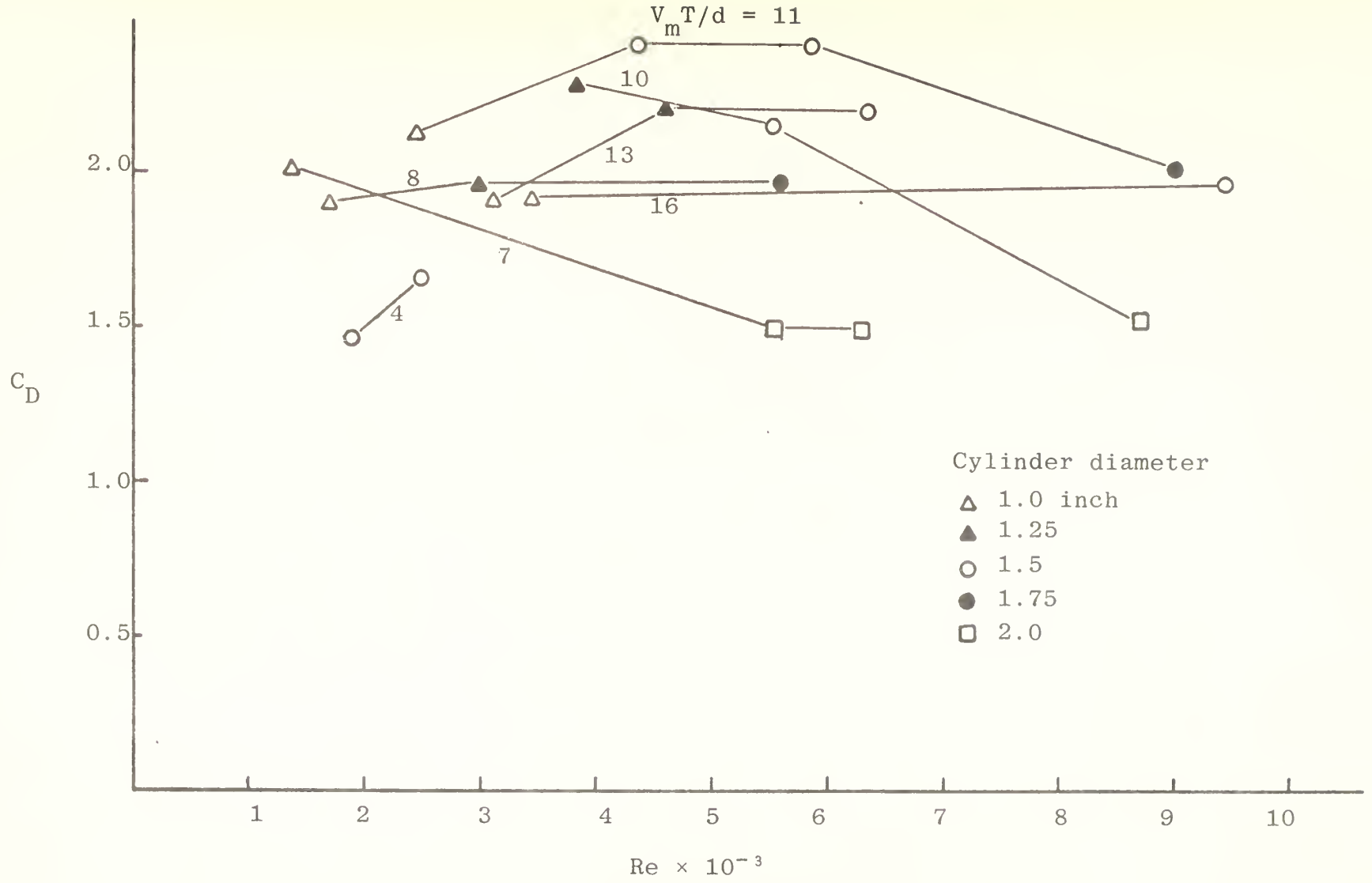

Figure 22. C_D versus Reynolds number for cylinders.

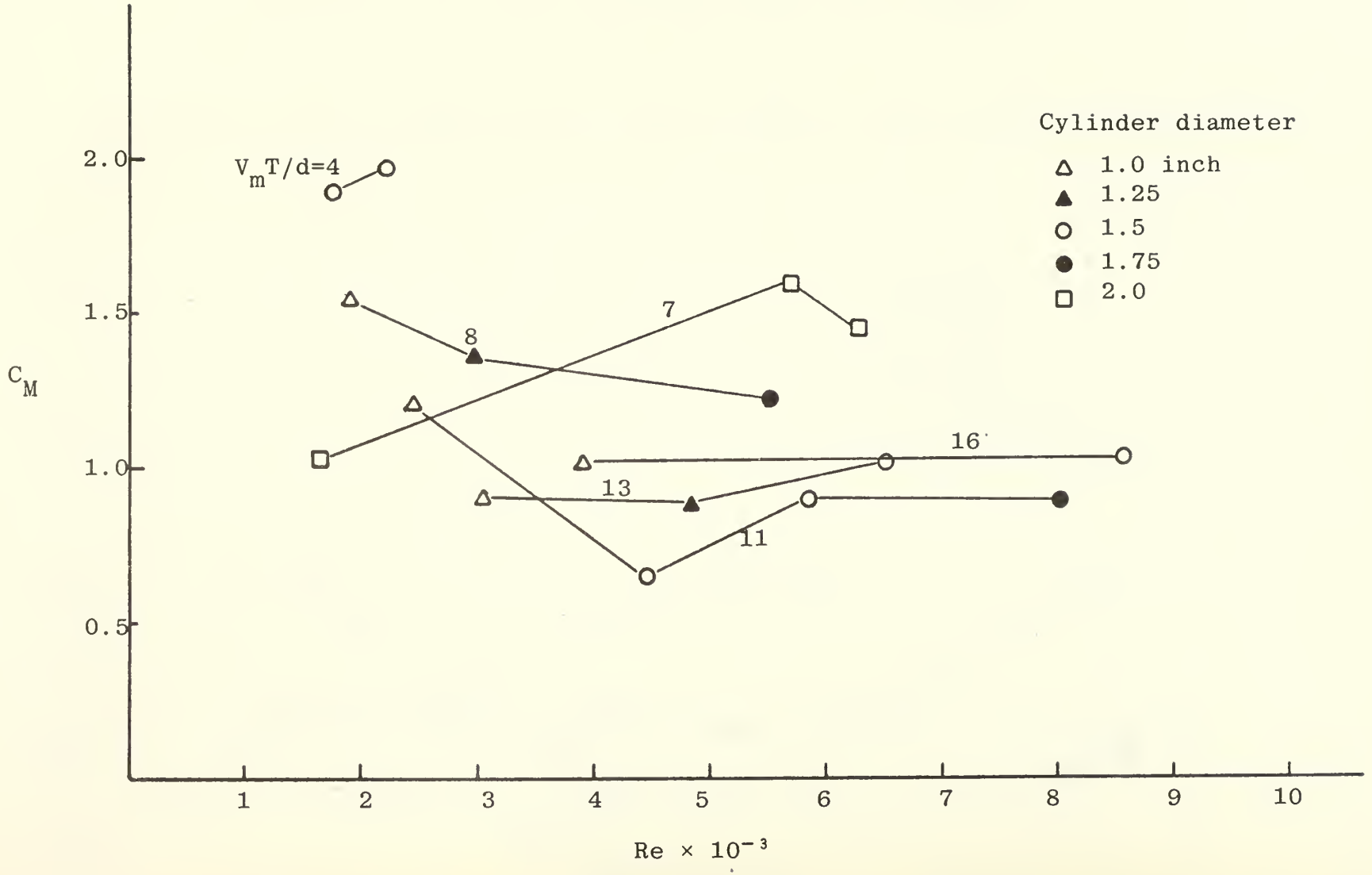

Figure 23. C_M versus Reynolds number for cylinders.

upon Reynolds number within the range of Reynolds numbers investigated.

B. SPHERE DATA

The inertia and drag coefficients calculated through the use of equations (29) and (30) are presented in figures 24 and 25. The inertia coefficient starts at its theoretical value of 1.5 and gradually drops to about unity for $V_m T/d \simeq 15$. The sphere data show considerably less scatter than those for the cylinder. Apparently, the added mass coefficient of a sphere in periodic flow could drop below its theoretical value of 0.5 for $V_m T/d$ larger than 15.

The drag coefficient shown in figure 25 gradually rises to about 0.8 at $V_m T/d \simeq 18$ and then decreases very slowly with increasing values of the period parameter. Comparison of the C_M and C_D values with those obtained with the cylinder shows that whereas in the case of cylinder C_M exhibits a minimum at about $V_m T/d = 12$, in the case of spheres, it decreases gradually, as noted above. On the other hand, C_D values follow similar trends.

The dependence of C_M and C_D on the Reynolds number was investigated by plotting both coefficients as a function of the Reynolds number for various values of $V_m T/d$. (See figures 26 and 27). Apparently, neither of the two coefficients depend upon the Reynolds number within the range of Reynolds numbers investigated.

The percent error λ^* given by equation (35) was calculated for the sphere and is presented in figure 28.

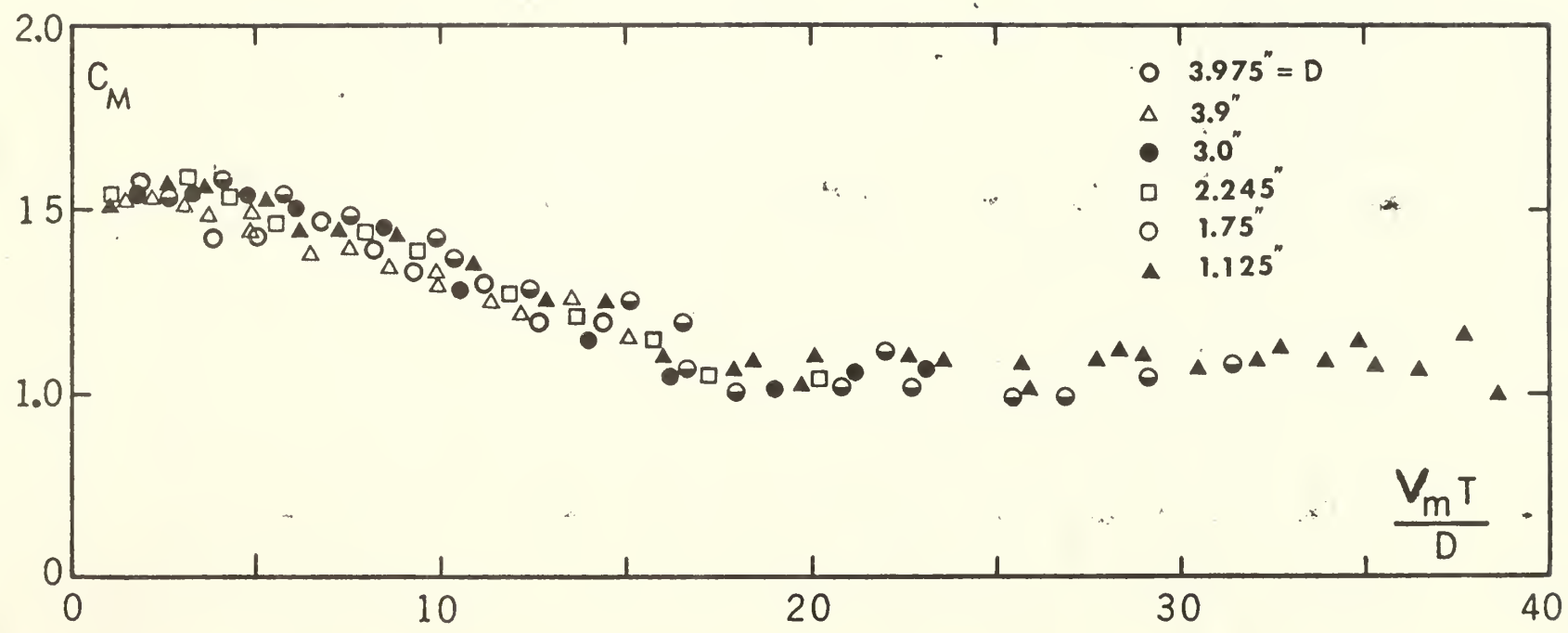

Figure 24 C_M versus the period parameter for spheres

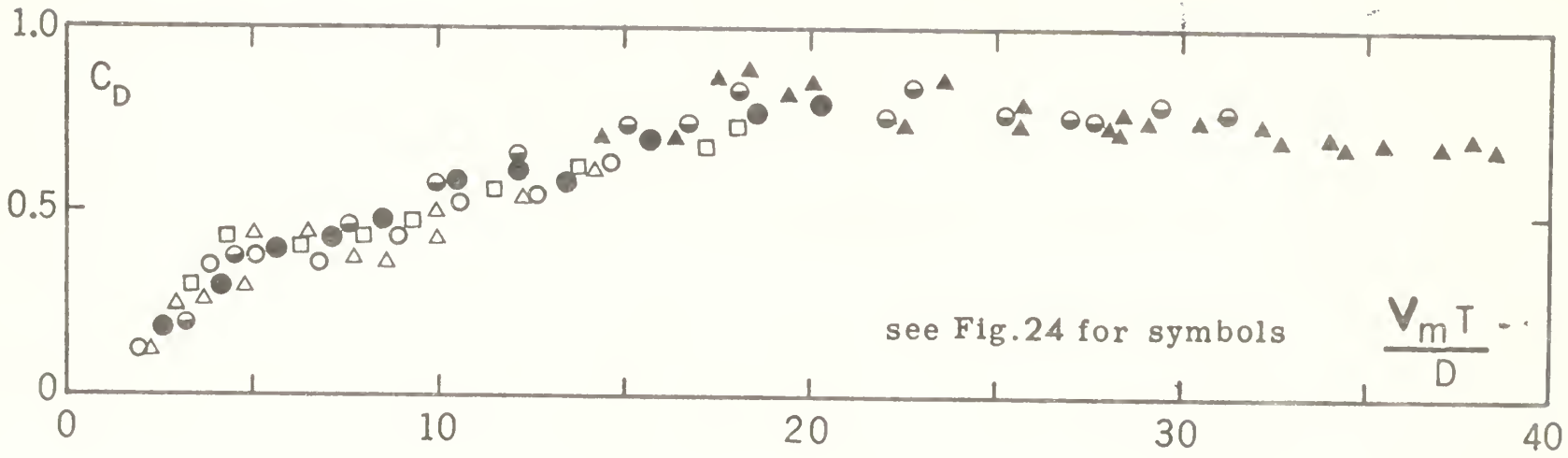

Figure 25 C_D versus the period parameter for spheres

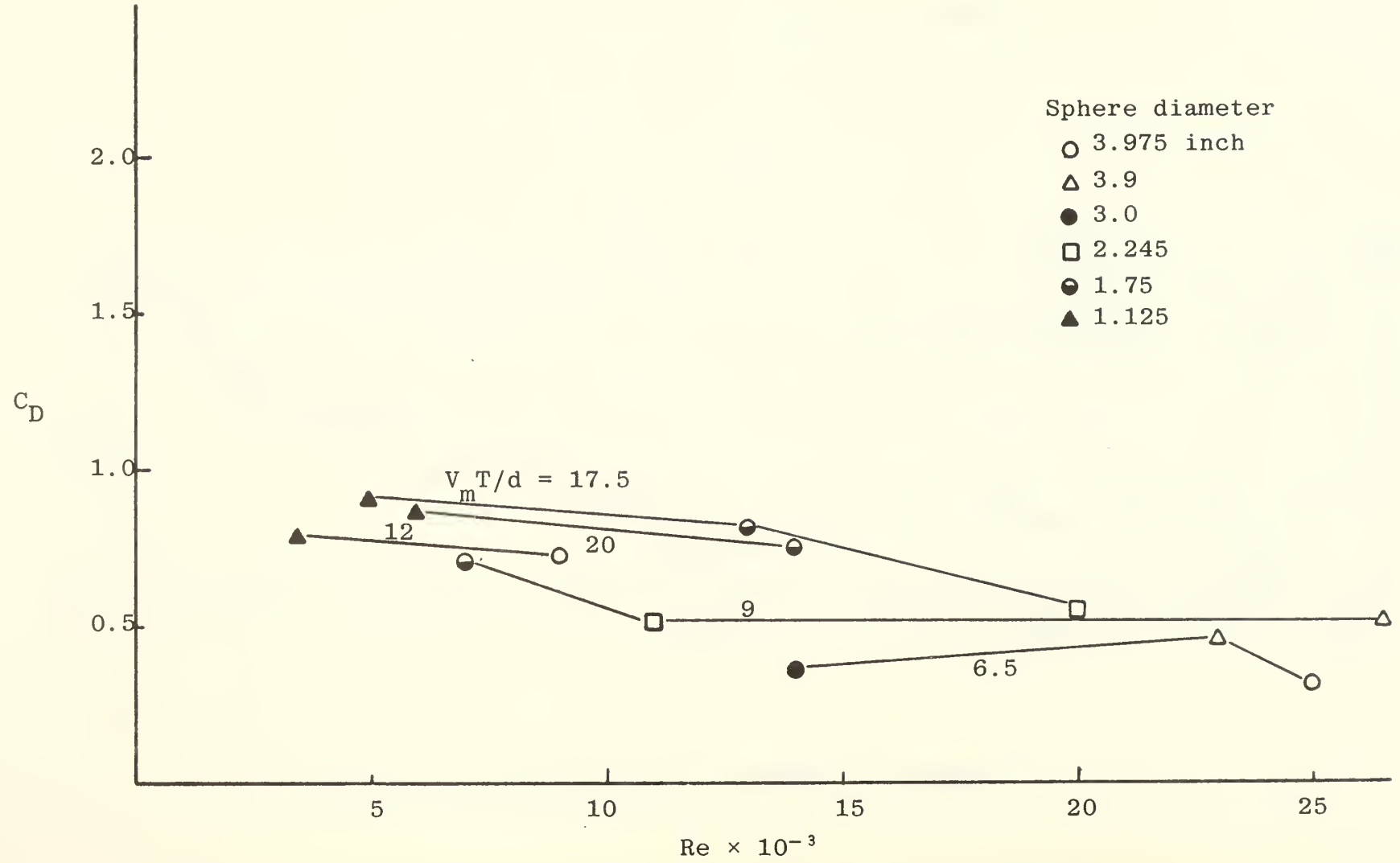

Figure 26. C_D versus Reynolds number for spheres.

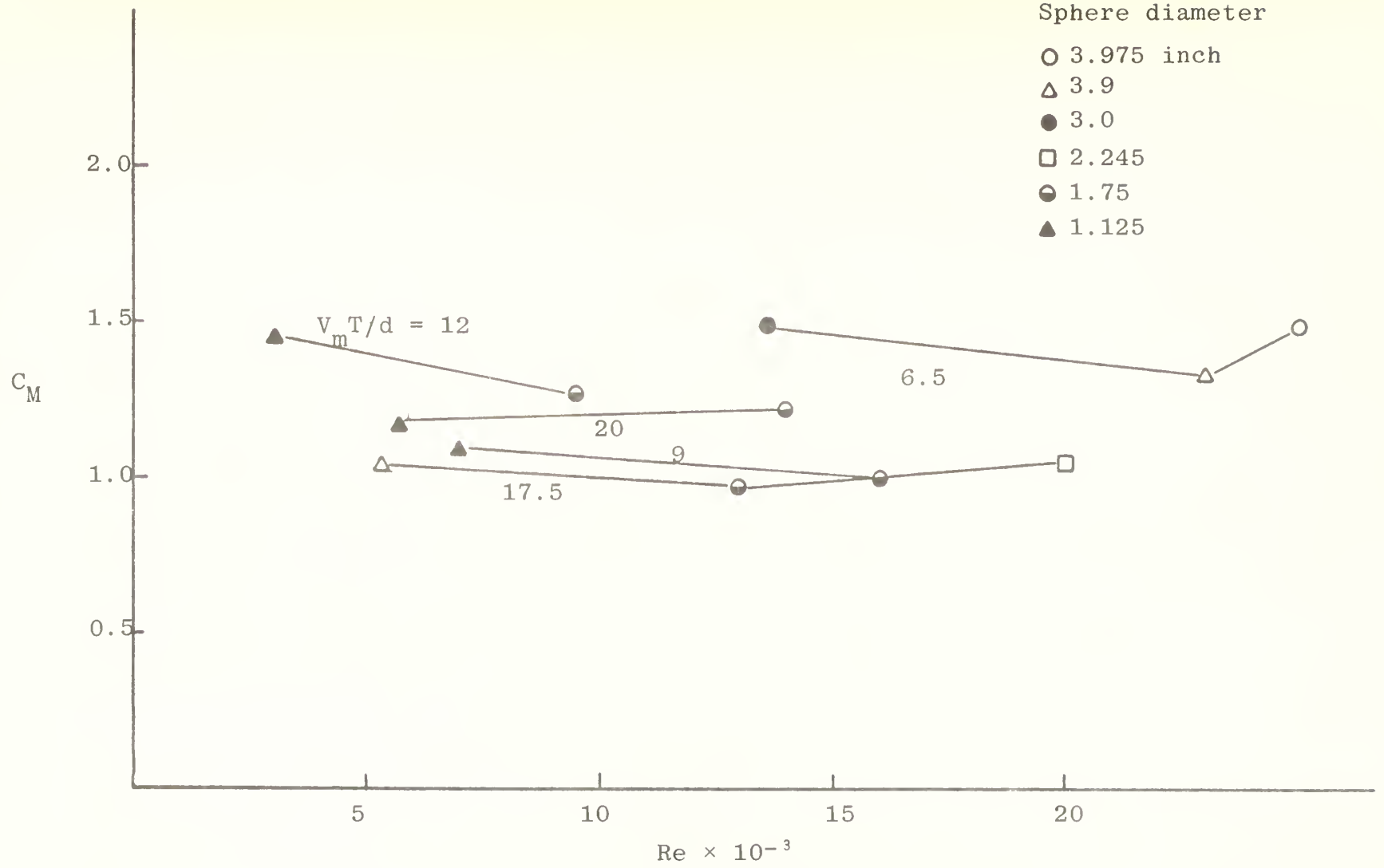

Figure 27. C_M versus Reynolds number for spheres.

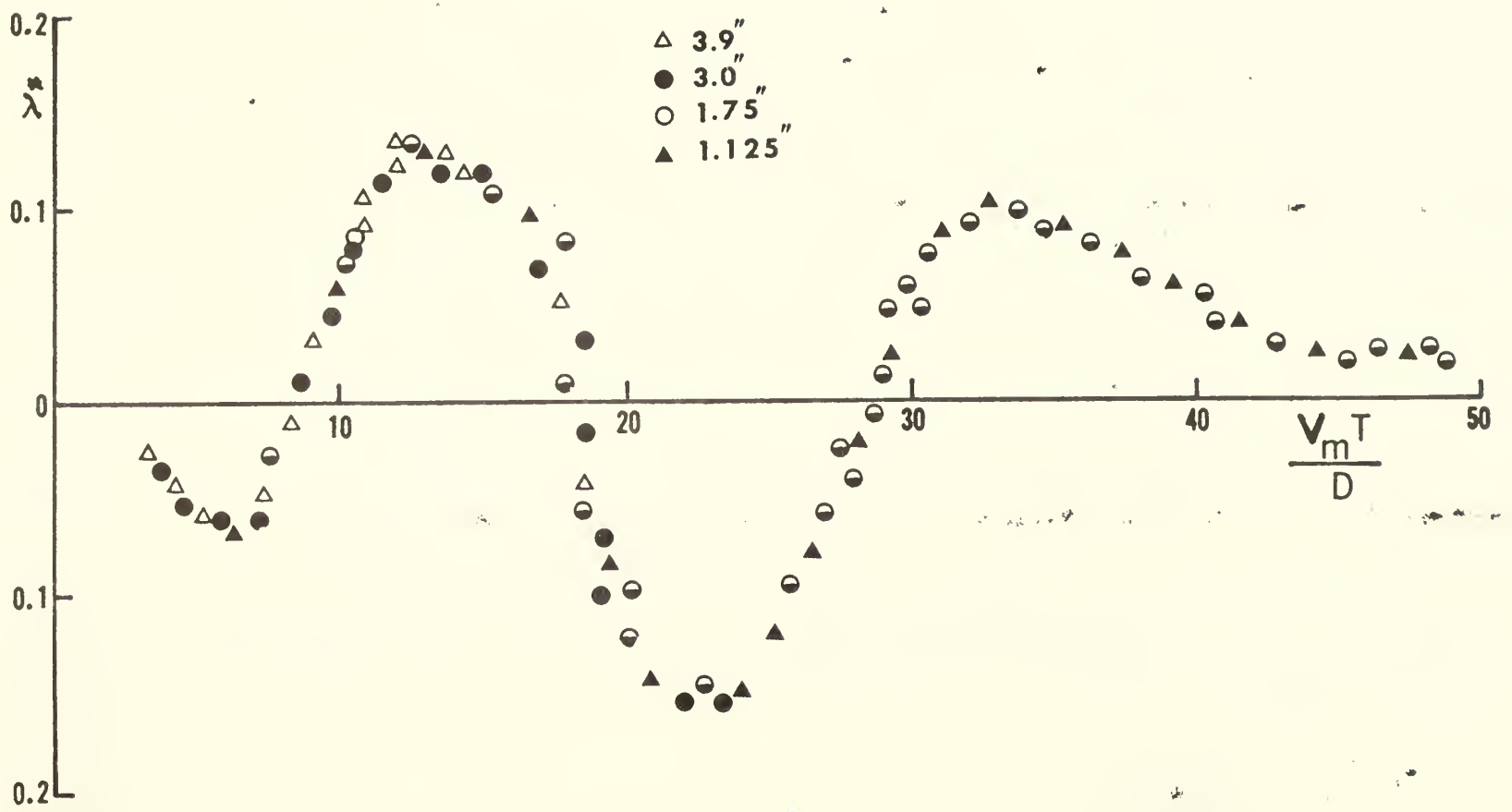

Figure 28 Error based on the maximum force versus the period parameter for spheres

Evidently the maximum value of λ^* may be as high as 15% at $V_m T/d$ values of about 12 and 22. The reasons for the occurrence of the maximum errors at the particular $V_m T/d$ values is not easy to explain. The first maximum takes place at the $V_m T/d$ value where both the drag and inertial forces are quite significant and the maximum force is nearly 100 degrees out of phase with the maximum velocity as seen in figure 29. The second absolute maximum of λ^* occurs at a $V_m T/d$ value where the maximum force and the maximum velocity are nearly in phase.

Finally, the variation of C_D with C_M is shown in figure 30. The data show a trend similar to that presented for the cylinder. Although, these coefficients are averaged over a cycle and thus do not represent their instantaneous variations over a cycle, the existence of a unique relationship between them is evidenced by figure 30.

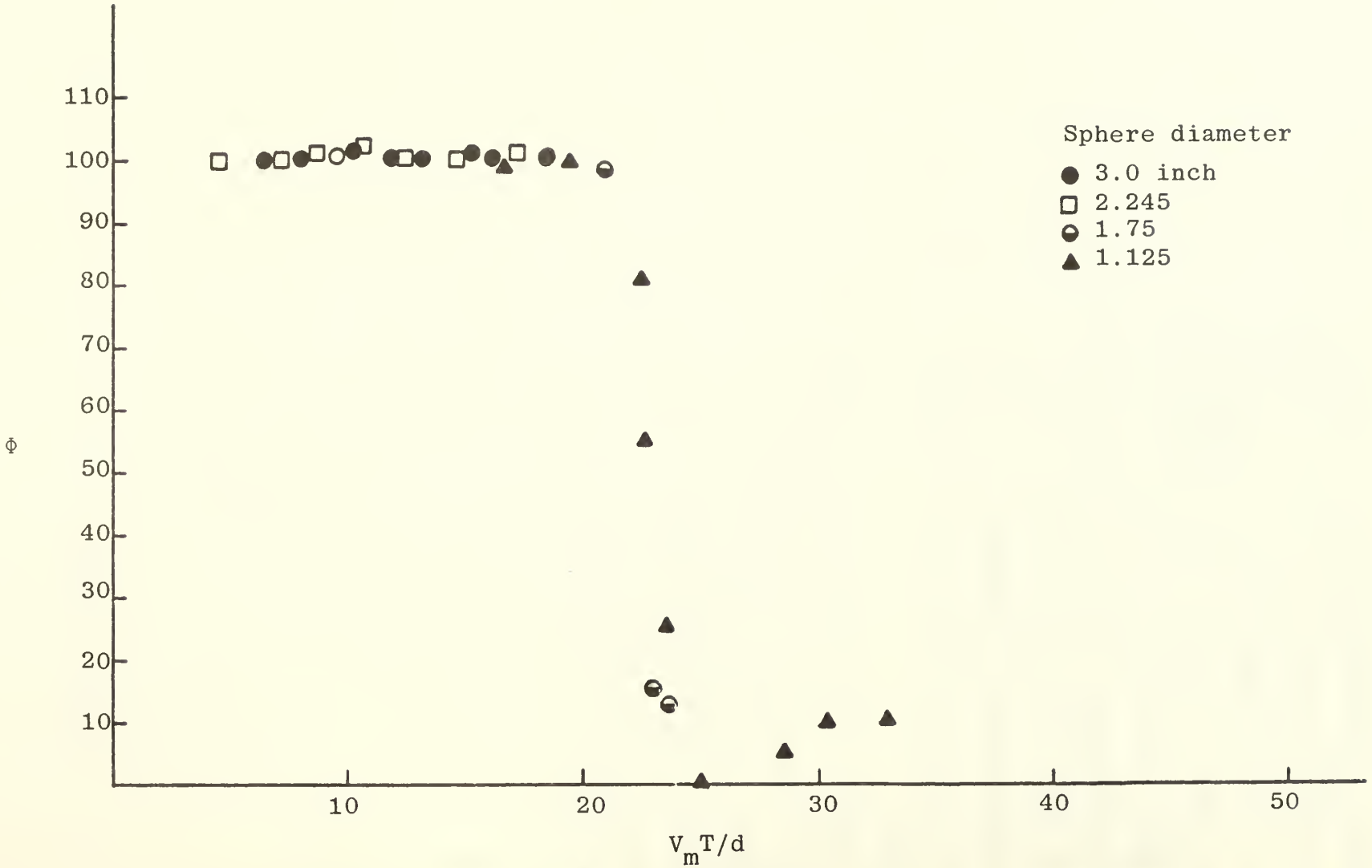

Figure 29. Phase angle versus period parameter for spheres.

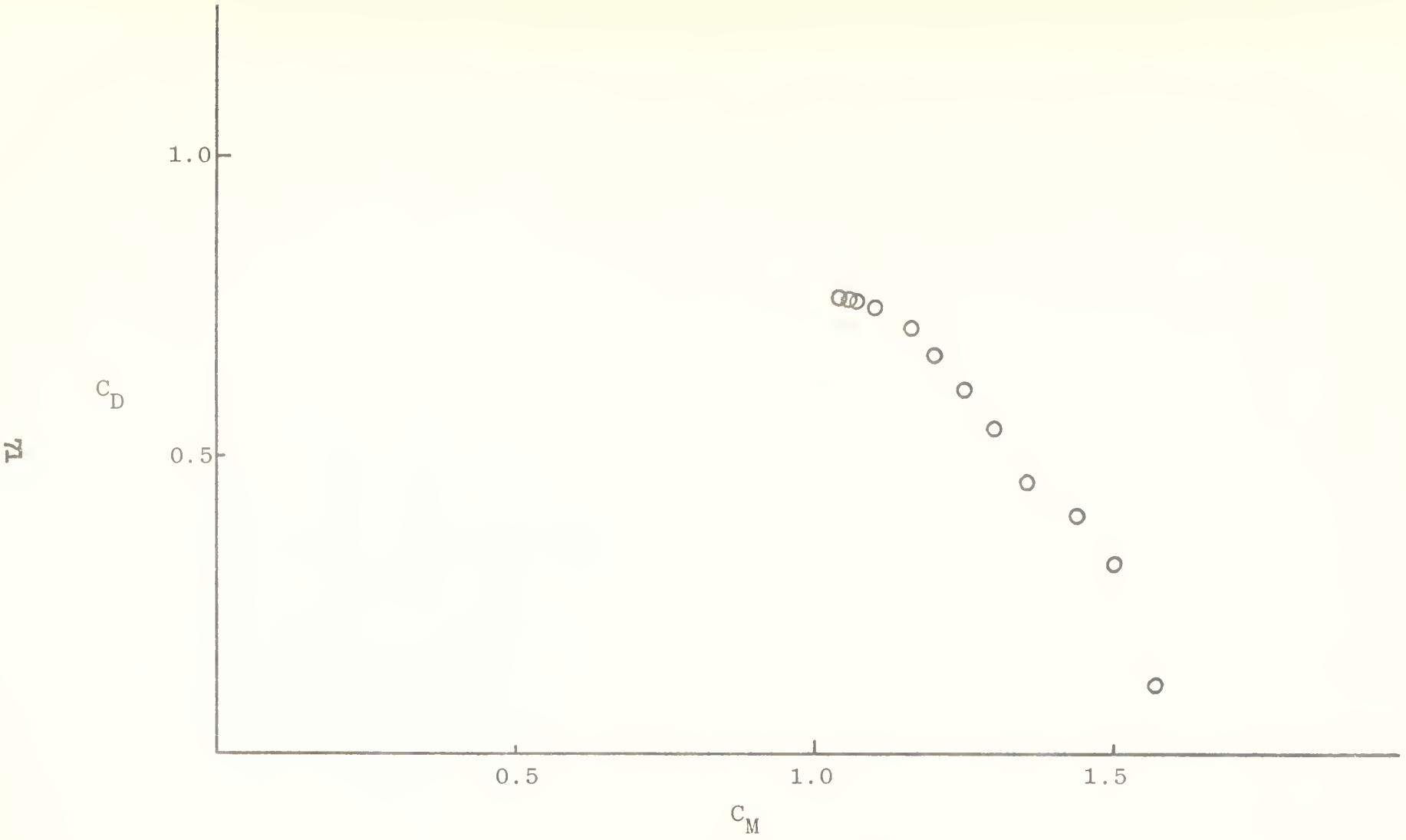

Figure 30. C_D versus C_M spheres.

V. CONCLUSIONS

The data presented herein warrant the following conclusions:

1) A U-shaped channel is ideally suited for the generation of perfectly harmonic flow oscillations about bluff bodies. Even though the period of the oscillations must be kept constant, the variability of the amplitude of oscillations and the size of the test bodies enable one to vary the basic parameters of the investigation. Furthermore, some of the difficulties (e.g. undesirable vibrations, the separation of the inertia of the test body, etc.) encountered in the experiments conducted by oscillating the test bodies are completely eliminated.

2) The drag and the inertia coefficients obtained for the circular cylinder follow in essence those obtained by Keulegan and Carpenter. The present data are considered to be more accurate and reliable, particularly for the inertia coefficient, than those obtained by Keulegan and Carpenter.

3) The finding that there is no noticeable correlation between the Reynolds number and the drag and inertia coefficients confirms the similar conclusion reached by Keulegan and Carpenter within the range of Reynolds numbers encountered.

4) The above conclusions which mainly concern the confirmation of Keulegan and Carpenter's historic data raise the important question that the scatter noted in the C_M and

C_D values obtained from the experiments conducted in ocean and noted by Wiegel [Ref. 36] may not be entirely due to the difficulty of the experimentation or due to the experimental errors. The scatter may rather be due to an additional factor not present either in Keulegan and Carpenter's work or in the present work. It may be conjectured that the effect of the ever present ocean currents on wave-generated oscillatory flow and possibly very large Reynolds numbers, for which the flow may become critical and the boundary layer about the body turbulent, may be responsible for the observed scatter. This aspect of the problem is currently being investigated through the use of an oscillating flow water tunnel.

5) The most important and previously unexplored finding of the present investigation is that the lift or the transverse force is as large as the in-line force. The frequency of the alternating force depends on $V_m T/d$ and various frequencies may occur in a given cycle. These frequencies may occur at the frequency of the flow oscillations and at two, three or four times the flow oscillations. It is also possible that additional harmonics may be superimposed on these oscillations. These findings make it mandatory that the forces acting on cylinders be calculated by considering the vectorial sum of the in-line and transverse forces. One must also consider various frequencies of oscillation in assessing the fatigue characteristics and the structural integrity of piles.

6) In view of the significant contribution of the lift forces to the total force one must also raise the question as to whether undue amount of effort and attention have been given in the past to the determination of the components of the in-line force and to the use of the Morison equation for the prediction of the forces acting on cylinders when the transverse force is as much as or larger than the in-line force. It appears from the discussion of the total force coefficient that there is a fairly good correlation between the total force coefficient and V_mT/d. It also appears that the largest value of the said coefficient occurs at $V_mT/d \simeq 10$. The use of such a coefficient together with a knowledge of the frequency of lateral oscillations may be more meaningful than the use of the Morison equation which deals only with the prediction of the in-line forces.

7) The force coefficients for the sphere follow in general the same trends as noted for those for the in-line force acting on cylinders. No attempt was made to measure the lateral forces acting on spheres. Apparently, these are more random in nature and thus more difficult to couple with the in-line forces to determine a total force coefficient in terms of V_mT/d. The sphere data, like the cylinder data, show that there is no correlation between the force coefficients and the Reynolds number within the range of Reynolds numbers investigated.

VI. RECOMMENDATIONS FOR FURTHER STUDIES

In view of the success achieved with the oscillatory flow channel used in the present investigation it is recommended that the experiments by extended to higher Reynolds numbers (approximately 10^6) in a similar but larger channel and the in-line and transverse forces be measured and analyzed in the same manner for cylinders, spheres and plates placed not only in the middle of the test section but also close to one of the walls of test section. The latter type of experiments will increase our understanding of the forces acting on large pipe lines, placed on or near the ocean bottom.

APPENDIX A

Computer Programs

```
CCCCCCCCCCCCCCCCCCCCCCCCCCCCCCCCCCCCCCCCCCCCCCCCCCCCCCCCCCCCCCCCCCCCCCCC
C                                                                      C
C      AVERAGE CD AND CM CALCULATIONS FOR CYLINDERS                    C
C                                                                      C
C      TIME=DIMENSIONLES TIME (TIME/PERIOD)                            C
C      BETA=DIMENSIONLES DISPLACEMENT(UMAX*PER/DIA)                    C
C      CL=CYLINDER LENGTH IN FEET                                      C
C      DIA=DIAMETER OF CYLINDER IN FEET                                C
C      AMP=AMPLITUDE OF MOTION IN FEET                                 C
C      PER=PERIOD IN SECS (CHART PERIOD/CHARTSPEED)                    C
C      ZI=FORCE COEFFICIENTS                                           C
C      CM=INERTIA COEFFICIENT                                          C
C      CD=DRAG COEFFICIENT                                             C
C      REMF=REMAINDER FUNCTION                                         C
C      AI,BI=FOURIER COEFFICIENTS                                      C
C      N=NUMBER OF DATA SETS                                           C
C      CN=CONVERTION FACTOR                                            C
C                                                                      C
CCCCCCCCCCCCCCCCCCCCCCCCCCCCCCCCCCCCCCCCCCCCCCCCCCCCCCCCCCCCCCCCCCCCCCCC

      G=32.174
      RHO=62.4/G
      PI=3.14159
      CNU=0.0000105
      CL=1.4946
C
C     INITIATE DATA SETS
C
      N=1
      DO 100 I=1,N
C
C     READ IN PARAMETERS WHICH CHARACTERIZE THE DATA SET
C
      READ(5,10)DIA,AMP,PER,NCARD,UMX,CN
C
C     COMPUTE FORCE COEFFICIENTS
C
      Z1=2*PER**2/(PI**3*DIA**2*CL*RHO*AMP)
      Z2=-3*PER**2/(8*RHO*DIA*PI*CL*AMP**2)
C
C     COMPUTE BETA
C
      BETA=2*PI*AMP/DIA
C
C     COMPUTE REYNOLDS NUMBER
C
      REYNO=(UMX*DIA)/CNU
C
C     PRINT OUT PARAMETERS AND COEFFICIENTS
C
      WRITE(6,15)DIA,AMP,PER,Z1,Z2,UMX,CN
      WRITE(6,20)
      TIME=0.0
      CM=0.0
      CD=0.0
      DELTAT=0.034965
C
C     START DATA REDUCTION
C
      DO 200 J=1,NCARD
      READ(5,25)F
      F=CN*F
      ALPHA=2*PI*TIME
      SINA=SIN(ALPHA)
      COSA=COS(ALPHA)
      FSINA=DELTAT*F*SINA
      FCOSA=DELTAT*F*COSA
      CM=FSINA+CM
```

```
      CD=FCOSA+CD
C
C     PRINT OUT COMPONENTS FOR DRAG AND INERTIA COEFFICIENT
C
      WRITE(6,30)TIME,ALPHA,COSA,SINA,F,FCOSA,FSINA
      TIME=TIME+DELTAT
  200 CONTINUE
      CM=Z1*CM
      CD=Z2*CD
      WRITE(6,35)
      WRITE(6,40)CM,CD,BETA,REYNO
C
C     COMPUTE REMAINDER FUNC.
C
      ANGLE=0.0
      WRITE(6,45)
      TIME=0.0
      DO 300 K=1,NCARD
      READ(5,55)F
      F=CN*F
      THETA1=((2.0*PI)/360)*ANGLE
      C1=(ABS(COS(THETA1)))*COS(THETA1)
      C2=RHO*((UMX**2.0)/2.0)*DIA*CL
      C3=((PI**2)*DIA*SIN(THETA1))/(UMX*PER)
      F1=(CM*C3-CD*C1)
      F=F/C2
      REMF=F-F1
      WRITE(6,50)TIME,F,F1,REMF
      ANGLE=12.12938+ANGLE
      TIME=TIME+DELTAT
  300 CONTINUE
  100 CONTINUE
   10 FORMAT(3F10.4,I10,F10.4,F10.6)
   15 FORMAT('1',10X,'DIA=',F8.4,5X,'AMP=',F8.4,5X,'PER=',
     1F8.4,5X,'Z1=',F8.4,5X,'Z2=',F9.4,5X,'UMX=',F8.4,5X,
     2'CN=',F10.6)
   20 FORMAT('0',3X,'TIME/PER',7X,'ALPHA',7X,'COSA',8X,'SINA
     3',5X,'F',11X,'FCOSA',8X,'FSINA')
   25 FORMAT(F10.4)
   30 FORMAT('0',7F12.4)
   35 FORMAT('0',7X,'CM=',7X,'CD=',7X,'BETA=',7X,'REYNO=')
   40 FORMAT('0',4F12.4)
   45 FORMAT('0',7X,'TIME',9X,'F',9X,'F1',9X,'REMF')
   50 FORMAT('0',4F12.4)
   55 FORMAT(F10.4)
      STOP
      END
```

```
CCCCCCCCCCCCCCCCCCCCCCCCCCCCCCCCCCCCCCCCCCCCCCCCCCCCCCCCCCCCCCCCCCCC
C                                                                     C
C      AVERAGE CD AND CM CALCULATIONS FOR SPHERES                     C
C                                                                     C
C      TIME=DIMENSIONLES TIME (TIME/PERIOD)                           C
C      BETA=DIMENSIONLES DISPLACEMENT(UMAX*PER/DIA)                   C
C      DIA=DIAMETER OF SPHERE IN FEET                                 C
C      AMP=AMPLITUDE OF MOTION IN FEET                                C
C      PER=PERIOD IN SECS (CHART PERIOD/CHARTSPEED)                   C
C      ZI=FORCE COEFFICIENTS                                          C
C      CM=INERTIA COEFFICIENT                                         C
C      CD=DRAG COEFFICIENT                                            C
C      REMF=REMAINDER FUNCTION                                        C
C      AI,BI=FOURIER COEFFICIENTS                                     C
C      N=NUMBER OF DATA SETS                                          C
C      CN=CONVERTION FACTOR                                           C
C                                                                     C
CCCCCCCCCCCCCCCCCCCCCCCCCCCCCCCCCCCCCCCCCCCCCCCCCCCCCCCCCCCCCCCCCCCC

      G=32.174
      RHO=62.4/G
      PI=3.14159
      CNU=0.0000105
C
CC    INITIATE DATA SETS
C
      N=1
C
CC    READ IN PARAMETERS WHICH CHARACTERIZE THE DATA SET
C
      DO 100 I=1,N
      READ(5,10)DIA,AMP,PER,NCARD,UMX,CN
C
CC    COMPUTE FORCE COEFFICIENTS
C
      Z1=3*PER**2/((PI**3)*(DIA**3)*RHO*AMP)
      Z2=-3*PER**2/(2*RHO*(PI**2)*(DIA**2)*(AMP**2))
C
CC    COMPUTE BETA
C
      BETA=2*PI*AMP/DIA
C
CC    COMPUTE REYNOLDS NUMBER
C
      REYNO=(UMX*DIA)/CNU
C
CC    PRINT OUT PARAMETERS AND COEFFICIENTS
C
      WRITE(6,15)DIA,AMP,PER,Z1,Z2,UMX,CN
      WRITE(6,20)
      TIME=0.0
      CM=0.0
      CD=0.0
      DELTAT=0.034965
C
CC    START DATA REDUCTION
C
      DO 200 J=1,NCARD
      READ(5,25) F
      F=CN*F
      ALPHA=2*PI*TIME
      SINA=SIN(ALPHA)
      COSA=COS(ALPHA)
      FSINA=DELTAT*F*SINA
      FCOSA=DELTAT*F*COSA
      CM=FSINA+CM
      CD=FCOSA+CD
C
CC    PRINT OUT COMPONENTS FOR DRAG AND INERTIA COEFFICIENT
C
      WRITE(6,30)TIME,ALPHA,COSA,SINA,F,FCOSA,FSINA
      TIME=TIME+DELTAT
```

```
200 CONTINUE
    CM=Z1*CM
    CD=Z2*CD
    WRITE(6,35)
    WRITE(6,40)CM,CD,BETA,REYNO
100 CONTINUE
 10 FORMAT(3F10.4,I10,F10.4,F10.6)
 15 FORMAT('1',10X,'DIA=',F8.4,5X,'AMP=',F8.4,5X,'PER=',
   1F8.4,5X,'Z1=',F8.4,5X,'Z2=',F9.4,5X,'UMX=',F8.4,5X,
   2'CN=',F10.6)
 20 FORMAT('0',3X,'TIME/PER',7X,'ALPHA',7X,'COSA',8X,'SINA
   3',5X,'F',11X,'FCOSA',8X,'FSINA')
 25 FORMAT(F10.4)
 30 FORMAT('0',7F12.4)
 35 FORMAT('0',7X,'CM=',7X,'CD=',7X,'BETA=',7X,'REYNO=')
 40 FORMAT('0',4F12.4)
    STOP
    END
```

```
CCCCCCCCCCCCCCCCCCCCCCCCCCCCCCCCCCCCCCCCCCCCCCCCCCCCCCCCCCCCCCCCCCC
C     MAX. LIFT COEFFICIENT CALCULATION                             C
C     FOR CYLINDERS                                                 C
C                                                                   C
C     CMLC= MAX. LIFT COEFFICIENT                                   C
C     UMX= MAX. VELOCITY                                            C
C     F=MEASURED LIFT FORCE                                         C
C     CF= CALIBRATION FACTOR FOR FORCE                              C
C     Z= ELEVATION                                                  C
C     CZ= CALIBRATION FACTOR FOR ELEVATION                          C
C     CL= LENGTH OF THE CYLINDER                                    C
C     DIA= DIAMETER OF THE CYLINDER                                 C
C     BETA=MAX.VELOCITY*PERIOD/DIAMETER                             C
C                                                                   C
CCCCCCCCCCCCCCCCCCCCCCCCCCCCCCCCCCCCCCCCCCCCCCCCCCCCCCCCCCCCCCCCCCCC

      RHO=1.9394
      CL=1.4946
      PI=3.1415926
      K=2
      DO 200 J=1,K
      READ(5,1) DIA,CF,CZ,N
      WRITE(6,50)
      WRITE(6,10) DIA,CF,CZ,N
      WRITE(6,30)
      WRITE(6,40)
      DO 100 I=1,N
      READ(5,2) Z,F
      F=F*CF
      Z=(Z*CZ)/12.0
      UMX=2.1969179*Z
      BETA=UMX*2.86/DIA
      UMXSQ=(UMX**2)/2.0
      CMLC=F/(RHO*UMXSQ*DIA*CL)
      WRITE(6,20) BETA,F,CMLC,UMX,Z
  100 CONTINUE
  200 CONTINUE
    1 FORMAT(3F12.6,I4)
   10 FORMAT('0',10X,'DIA=',F8.6,5X,'CF=',F8.6,5X,'CZ=',F8.6
     1,5X,'N=',I2)
    2 FORMAT(2F12.6)
   20 FORMAT('0',10X,F6.2,10X,F8.6,10X,F6.3,25X,F6.4,10X,
     2F6.4)
   30 FORMAT('0')
   40 FORMAT('0',12X,'BETA',13X,'FL',14X,'CMLC',27X,'UMX',
     314X,'Z')
   50 FORMAT('0')
      STOP
      END
```

APPENDIX B

Error Results

$V_m T/d = 7.21$

t/T	λ
0.0	0.1808
0.0350	0.0802
0.0699	-0.0007
0.1049	-0.0063
0.1399	-0.0085
0.1748	0.0376
0.2098	-0.0204
0.2448	-0.0871
0.2797	-0.1508
0.3147	-0.1075
0.3496	0.0438
0.3846	0.2024
0.4196	0.3429
0.4545	0.3841
0.4895	0.2742
0.5245	0.1152
0.5594	0.1090
0.5944	0.1184
0.6294	0.1612
0.6643	0.1261
0.6993	0.1282
0.7343	0.1590
0.7692	0.2415
0.8042	0.1864
0.8392	0.1375
0.8741	-0.0165
0.9091	-0.0540
0.9441	0.0508
0.9790	0.1626

$V_m T/d = 11.79$

t/T	λ
0.0	0.1416
0.0350	0.1392
0.0699	0.0897
0.1049	0.0292
0.1399	-0.0146
0.1748	-0.0463
0.2098	-0.0687
0.2448	-0.1056
0.2797	-0.1725
0.3147	-0.1604
0.3496	-0.0407
0.3846	0.1512
0.4196	0.2489
0.4545	0.1882
0.4895	0.0412
0.5245	0.0215
0.5594	0.0408
0.5944	0.0813
0.6294	0.0798
0.6643	0.1240
0.6993	0.1042
0.7343	0.1653
0.7692	0.1867
0.8042	0.2226
0.8392	0.1327
0.8741	-0.0216
0.9091	-0.1294
0.9441	-0.0124
0.9790	0.1133

$V_m T/d = 17.26$

t/T	λ
0.0	0.0120
0.0350	0.0258
0.0699	-0.0174
0.1049	-0.1117
0.1399	-0.0922
0.1748	-0.0531
0.2098	-0.0383
0.2448	0.0406
0.2797	0.1073
0.3147	0.0754
0.3496	-0.0553
0.3846	-0.0829
0.4196	0.0692
0.4545	0.0745
0.4895	-0.0306
0.5245	-0.1331
0.5594	-0.2217
0.5944	-0.3000
0.6294	-0.2443
0.6643	-0.1767
0.6993	-0.1346
0.7343	-0.1083
0.7692	-0.1230
0.8042	-0.1435
0.8392	-0.0751
0.8741	-0.0519
0.9091	-0.1982
0.9441	-0.0822
0.9790	0.0441

$V_m T/d = 28.0$

t/T	λ
0.0	0.0336
0.0350	-0.0117
0.0699	-0.0259
0.1049	-0.0188
0.1399	-0.0499
0.1748	-0.0632
0.2098	-0.0646
0.2448	-0.0259
0.2797	0.0370
0.3147	-0.0047
0.3496	0.0201
0.3846	0.0968
0.4196	0.0642
0.4545	-0.0421
0.4895	-0.0211
0.5245	-0.1366
0.5594	-0.2056
0.5944	-0.2148
0.6294	-0.1989
0.6643	-0.1850
0.6993	-0.1611
0.7343	-0.1286
0.7692	-0.1396
0.8042	-0.1824
0.8392	-0.1464
0.8741	-0.1637
0.9091	-0.1100
0.9441	-0.0640
0.9790	0.0247

$V_m T/d = 42.69$

t/T	λ
0.0	0.0453
0.0350	-0.0276
0.0699	0.0294
0.1049	0.0178
0.1399	0.0138
0.1748	0.0120
0.2098	-0.0094
0.2448	-0.0234
0.2797	0.0405
0.3147	0.0150
0.3496	0.0503
0.3846	0.1239
0.4196	0.0555
0.4545	-0.0130
0.4895	0.0188
0.5245	-0.0454
0.5594	-0.1663
0.5944	-0.2912
0.6294	-0.1382
0.6643	-0.1558
0.6993	-0.1100
0.7343	-0.0568
0.7692	-0.0571
0.8042	-0.0893
0.8392	-0.0884
0.8741	-0.2306
0.9091	-0.1519
0.9441	-0.0727
0.9790	0.1086

LIST OF REFERENCES

1. Sarpkaya, T., "On Time-Dependent Flows of Incompressible Fluids," Developments in Mechanics, Midwestern Mechanics Conference, vol. 5, 1969, pp: 985-1001.

2. Stewartson, K., "The Theory of Unsteady Laminar Boundary Layers," Advances in Applied Mechanics, Ed. H.L. Dryden et alli., Academic Press, N.Y., vol. VI, 1960, pp: 1-37.

3. Stuart, J.T., "Unsteady Boundary Layers," Laminar Boundary Layers, Ed. L. Rosenhead, Oxford Univ. Press, Oxford, 1963, pp: 349-406.

4. Rott, N., "Theory of Time-Dependent Flows," Theory of Laminar Flows, Ed. F.K. Moore, Princeton Univ. Press, Princeton, 1964, pp: 395-438.

5. Stelson, T.E. and Mavis, F.T., "Virtual Mass and Acceleration in Fluids," Trans. ASCE, Paper No. 2870, 1955, pp: 518-530.

6. Sarpkaya, T., "Added Mass of Lenses and Parallel Plates," Jour. of Engineering Mechs. Div., ASCE, vol. 86, No. EM3, June 1960, pp: 141-152.

7. Mavis, T., "Virtual Mass of Plates and Discs in Water," ASCE Proc. Paper No. 7593, Oct. 1970, (See also discussion by C.J. Garrison in ASCE Proc. Paper No. 8012, April 1971, pp: 631-635).

8. Goldschmidt, V.W. and Protos, A., "Added Mass of Equilateral-Triangular Cylinders," Jour. of Engineering Mechs. Div. ASCE, EM6, Dec. 1968, pp: 1539-1545.

9. Hamilton, W.S. and Lindell, J.E., "Fluid Force Analysis and Accelerating Sphere Tests," Jour. of the Hydraulics Div. ASCE, HY6, June 1971, pp: 805-817.

10. Lord Rayleigh, "On the Motion of Solid Bodies Through Viscous Fluid," Phil. Mag. Series 6, Vol. 21, 1911, p. 697.

11. Odar, F. and Hamilton, W.S., "Forces on a Sphere Accelerating in a Viscous Fluid," Jour. of Fluid Mechs., Vol. 18, part 2, 1964, pp: 302-314.

12. Laird, A.D.K., "Water Forces on a Flexible Oscillating Cylinder," Jour. of Waterways and Harbors Div. ASCE, WW3, Paper No. 3234, 1963, pp: 125-137.

13. Laird. A.D.K., Johnson, C.A. and Walker, R.W., "Water Eddy Forces on Oscillating Cylinders," Trans. ASCE, Vol. 127, 1962, pp: 335-351.

14. Hamann, F. and Dalton, C., "The Forces on a Cylinder Oscillating Sinusoidally in Water," Jour. Engrg. Ind., Trans. ASME, Vol. 93B, 1971, pp: 1197-1203.

15. Roos, F.W. and Willmarth, W.W., "Some Experimental Results on Sphere and Disk Drag," AIAA, Vol. 9, No. 2, Feb. 1971, pp: 285-291.

16. Driscoll, J.R., Forces on Cylinders Oscillating in Water, Master's Thesis, Naval Postgraduate School, Monterey, Calif., 1972.

17. Morison, J.R., O'Brien, M.P., Johnson, J.W., and Schaaf, S.A., "The Force Exerted by Surface Waves on Piles," Petroleum Trans., AIME, Vol. 189, 1950, pp: 149-157.

18. Keulegan, G.H. and Carpenter, L.H., "Forces on Cylinders and Plates in an Oscillating Fluid," Journal of Research, NBS, Vol. 60, 1958, pp: 423-440.

19. Jen, Y., "Laboratory Study of Inertia Forces on a Pile," Jour. of Waterways and Harbors, Proc. ASCE, Vol. 94, WW1, 1968, pp: 59-76.

20. McNown, J.S., "Drag in Unsteady Flow," Proc. 9th International Congress of Applied Mechs., Vol. 3, Brussels, 1957.

21. McNown, J.S. and Keulegan, G.H., "Vortex Formation and Resistance in Periodic Motion," Proc. ASCE, vol. 85, No. EM1, 1959.

22. Brater, E.F., McNown, J.S., and Stair, L.D., "Wave Forces on Submerged Structures," Trans. ASCE, Paper No. 3182, 1958, pp: 661-696.

23. Garrison, C.J. and Snider, R.H., "Wave Forces on Large Submerged Tanks," Sea Grant Publications No. 210, Texas A & M University, Jan., 1970.

24. Iverson, H.W. and Balent, R., "A Correlating Modulus for Fluid Resistance in Accelerated Motion," Jour. of Applied Physics, vol. 22, 1951, p. 325.

25. Keim, S.R., "Fluid Resistance to Cylinders in Accelerated Motion," Proc. ASCE, Jour. of Hydraulics Div., vol. 82, Dec. 1956.

26. Laird, A.D.K., Johnson, C.A. and Walker, R.W., "Water Forces on Accelerated Cylinders," Jour. of Waterways and Harbors Div., ASCE, WW1, 1959, pp: 99-119.

27. Sarpkaya, T. and Garrison, C.J., "Vortex Formation and Resistance in Unsteady Flow," Jour. of Applied Mechs., vol. 30, Trans. ASME, vol. 85E, 1963, pp: 16-24.

28. Bishop, R.E.D. and Hassan, A.Y., "The Lift and Drag Forces on a Circular Cylinder Oscillating in a Flowing Fluid," Proc. of the Royal Society, London, Ser. A., vol. 272, 1964.

29. Chen, C.F. and Ballengee, D.B., "Vortex Shedding from Circular Cylinders in an Oscillating Freestream," AIAA Jour., vol. 9, No. 2, Feb. 1971, pp: 340-342.

30. Hatfield, H.M. and Morkovin, M.V., "Effect of an Oscillating Free Stream on the Unsteady Pressure on a Circular Cylinder," ASME Paper No. 72-WA/FE-12, 1972.

31. Mercier, J.A., A discussion of (Blevins, R., "Vortex Induced Vibration of Circular Cylindrical Structures," ASME Paper No. 72-WA/FE-39, 1972), presented at the 1972 Winter Annual Meeting of ASME, N.Y., 1972.

32. Davenport, A.G., "The Application of Statistical Concepts to the Wind Loading of Structures," The Institute of Civil Engineers, vol. 19, 1961, pp: 449-472.

33. Bidde, D.D., "Laboratory Study of Lift Forces on Circular Piles," Jour. of Waterways, Harbors and Coastal Engineering Div., ASCE, WW4, Nov., 1971, pp: 595-614.

34. Rance, P., "Wave Forces on Cylindrical Members of Structures," Hydraulics Research, 1969, pp: 14-17.

35. Grace, R.A. and Casciano, F.M., "Ocean Wave Forces on Subsurface Spheres," Jour. of the Waterways and Harbors Div., ASCE, Vol. 95, WW3, Proc. Paper No. 6722, August 1969, pp: 291-317.

36. Weigel, R.L., Oceanographical Engineering, Prentice Hall, Inc., Englewood Cliffs, N.J., 1964.

DISTRIBUTION LIST

		No. Copies
1.	Defense Documentation Center Cameron Station Alexandria, Virginia 22314	12
2.	National Science Foundation Washington, D. C. 20550	20
3.	Dean of Research Naval Postgraduate School Monterey, Calif. 93940	1
4.	Department Chairman, Code 59 Mechanical Engineering Naval Postgraduate School Monterey, Calif. 93940	1
5.	Library, Code 0212 Naval Postgraduate School Monterey, Calif. 93940	2
6.	Prof. T. Sarpkaya, Code 59SL Mechanical Engineering Naval Postgraduate School Monterey, Calif. 93940	20
7.	LT (J.G.) Olcay Tuter 20. Sokak No. 9/4 Bahcelievler Ankara Turkey	2
8.	Chief of Naval Research Arlington, Virginia 22217 Attn: (Appropriate branch within Office of Naval Research)	2
9.	Officer in Charge The Civil Engineering Laboratory (Attn: Code L-44) Naval Construction Battalion Center Port Hueneme, Calif. 93043	2